Science and Technology Indonesia
e-ISSN:2580-4391 *p*-ISSN:2580-4405
Vol. 11, No. 2, April 2026

Research Paper

Block Bootstrap for Spatiotemporal Data in Generalized Space Time Autoregressive (GSTAR)

Eni Sumarminingsih[1*], Rahma Fitriani[1], Darmanto[1], Eka Dani Maulana[1], Natasha Aulia[1], Luzar Dwain Ruszardi[1]

[1]*Department of Statistics, Universitas Brawijaya, East Java, 65145, Indonesia*
***Corresponding author**: eni_stat@ub.ac.id

Abstract
Generalized Space-Time Autoregressive is a model that can be used for data with spatial and temporal dependence. The GSTAR model is widely used in various phenomena such as rainfall, temperature, inflation, and others. GSTAR assumes normality of errors and non-autocorrelation. If the assumption of normality of errors is not met, then inference on parameters cannot be made. One solution to this problem is to use bootstrapping. However, bootstrapping for spatiotemporal data in the GSTAR model has not been developed. Therefore, this study aims to develop a bootstrapping method for spatiotemporal data in the GSTAR model. This development is done by adapting bootstrapping methods for time series data, namely, the non-overlapping block bootstrap (NBB) and the moving block bootstrap (MBB). This research continued with a series of simulations to evaluate the performance of the block bootstrap method as the number of observations, block length, and number of bootstrap replications were varied. Furthermore, the method's effectiveness was tested using rainfall data from Malang Regency. Simulation results show that both resampling schemes satisfy the asymptotic condition, where the bias decreases monotonically with increasing sample size (T) and block length. MBB consistently produces lower bias than NBB due to its more intensive use of overlapping data, which effectively reduces boundary effects. Although inference on autoregressive parameters can be accurate, inference on spatial autoregressive parameters yields less satisfactory results, indicating the limitations of time blocks in capturing complex spatial dependencies. Increasing the number of replications above B=100 does not significantly improve the precision of the variance estimate, indicating computational efficiency at that threshold. The t-test results confirm that there is no statistically significant difference in performance between NBB and MBB. Nevertheless, MBB is more recommended for practical applications due to its higher information density and better estimation stability.

Keywords
Spatiotemporal Data, Generalized Space Time Autoregressive (GSTAR), Block Bootstrap

Received: 31 December 2025, Accepted: 8 March 2026
https://doi.org/10.26554/sti.2026.11.2.701-731

1. INTRODUCTION

The Generalized Space-Time Autoregressive (GSTAR) model is used to analyze time-series data that exhibit spatial dependencies across locations. This model can be used to model phenomena such as rainfall (Iriany et al., 2013), air temperature (Aprianti et al., 2024; Zewdie et al., 2018), inflation (Hestuningtias and Kurniawan, 2023), GDP (Nurhayati et al., 2012), Covid-19 case (Huda and Imro'ah, 2023; Mukhaiyar et al., 2021), Dengue Fever case (Mukhaiyar et al., 2019), the amount of monthly crime activity (Masteriana et al., 2019), and so on. The GSTAR model was developed by Ruchjana (2002), with parameter estimation using the Ordinary Least Squares method (Ruchjana et al., 2012). Currently, there have been many developments of GSTAR models, such as GSTARX-GLS (Suhartono et al., 2016), GSTAR-Kalman Filter (Prillantika et al., 2018), GSTAR-SUR (Iriany et al., 2013), S-GSTAR-SUR (Setiawan et al., 2016), GSTAR-Kriging (Abdullah et al., 2018), GSTAR-ARCH (Nainggolan and Titaley, 2017), GSTAR with Heteroscedastic Effects (Mukhaiyar and Ramadhani, 2022), GSTAR with outlier Mukhaiyar et al. (2020) and many more. Several researchers developed GSTAR from the perspective of the spatial weights used, such as (Huda and Imro'ah, 2023; Mukhaiyar et al., 2021, 2024; Yundari et al., 2018).

The GSTAR model assumes normality of errors and non-autocorrelation. If the assumption of normality of errors is not met, it will result in invalid parameter significance tests. One solution to this problem is to perform bootstrapping. Bootstrapping is a method for estimating the sampling distribution of a statistic (such as the mean, median, variance, or regres-

sion coefficient) by repeatedly sampling with replacement from an existing data sample (the original sample). This bootstrap distribution is used to draw conclusions, such as: estimating the standard error of a statistic, constructing confidence intervals, and conducting hypothesis testing (Efron and Tibshirani, 1993). The bootstrap procedure begins with an original data sample of size n, which is assumed to represent the underlying population distribution. The next step is to repeatedly resample (e.g., B=1,000 times) by drawing new samples of size n from the original sample with replacement. Each new sample is called a bootstrap sample. After each bootstrap sample is drawn, the statistic of interest (such as the mean, median, or regression coefficient) is calculated from that bootstrap sample. After B iterations, we end up with a collection of B values of the statistic. This collection of values then forms the empirical bootstrap distribution of the statistic. This bootstrap distribution is then used for inference, such as estimating the standard error of the statistic (based on the bootstrap distribution's standard deviation) or constructing nonparametric confidence intervals.

However, bootstrapping time series data differs slightly from the traditional bootstrap. While with independent data we can shuffle the data individually, with time series we must preserve temporal dependencies (time order) to preserve the data's characteristics. Time series data exhibits autocorrelation, where today's values are highly dependent on yesterday's values. If we shuffle the data individually, this temporal relationship structure will be destroyed, and the analysis results will be invalid. Bootstrap procedures for time series data have been developed by Bergström (2018); Härdle et al. (2001); Kreiss and Lahiri (2012); Politis (2003). Bootstrap procedures for time series data include non-overlapping block bootstrap, moving block bootstrap, circular block bootstrap, and stationary bootstrap. Several studies on bootstrapping spatiotemporal data or models have been conducted by researchers such as Dumanjug et al. (2010); Feng et al. (2024). However, there are many types of spatiotemporal models, research Dumanjug et al. (2010) uses a model developed byLandagan and Barrios (2007) Where in the model y_{it} is a function of X_{it} which is an independent variable at location i at time t and w_{it} which is a spatial indicator at location i and time t. Feng et al. (2024) uses a model in which y_{it} is a function of the SAR effect, dynamic effect, lagged spatial effect, and Spatial Error effect. Currently, no one has developed bootstrapping on the GSTAR model. There are two bootstrapping approaches used in Dumanjug et al. (2010): the Non-parametric Residual Bootstrap approach and the block bootstrap approach, which is an adaptation of the block bootstrap to time series data. However, the bootstrap block developed by Dumanjug et al. (2010) differs from the bootstrap block for time-series data in general. In the study by Dumanjug et al. (2010), after the block is formed, parameter estimation is carried out within each block, and the resulting parameter estimators are then averaged. In Feng et al. (2024), the bootstrap method used is a weighted/residual bootstrap. This study develops a block bootstrap on spatiotemporal data using the GSTAR model.

In standard GSTAR inference, test statistics (such as the t-test) rely heavily on normally distributed errors for p-value validity. In complex spatio-temporal data, residuals often exhibit heavy tails or skewness, which makes parametric confidence intervals too narrow or misleading. Both the MBB and NBB can form the distribution of the parameter estimator. From the distribution of the parameter estimator, the expected value (mean) of the estimator, its standard error, and the confidence interval (constructed from the 2.5^{th} and 97.5^{th} percentiles) can be obtained, which can be used to make inferences about GSTAR parameters.

Similar to the inherent dependencies within time series data, spatiotemporal data exhibits correlations across both temporal and spatial dimensions. The block bootstrap method, a well-established approach for preserving such dependencies in time series analysis, is extended in this study to account for these dual relationships.

GSTAR has been widely used for modeling in various fields, but some studies only use normality plots for diagnostic checking (Masteriana et al., 2019; Nurhayati et al., 2012). Some studies even fail to check the assumption of normality of errors, such as Zewdie et al. (2018). However, the effect of abnormal errors is to invalidate statistical decision-making, such as in hypothesis testing or confidence interval construction. With the bootstrap block in GSTAR developed in this study, researchers can construct empirical distributions of parameter estimators based on field data characteristics, thereby forming confidence intervals for parameters that can also be used for hypothesis testing. Furthermore, the bootstrap block ensures that the spatial (neighbor) relationship and the temporal (autocorrelation) relationship are not broken during the resampling process.

Consequently, the purpose of this study is to develop a block bootstrap method for spatiotemporal data, with a primary focus on the GSTAR model. Simulations are then conducted to assess the performance of the block bootstrap method as a function of the number of observations, block length, and number of bootstrap replications. Furthermore, the application of rainfall data in Malang Regency is also demonstrated.

2. EXPERIMENTAL SECTION

2.1 Materials

The data used in this study are simulated data generated following the GSTAR (1,1) model with three locations and uniform weights. This study used uniform spatial weighting, inverse distance, and normalized cross-correlation. However, the normalized cross-correlation weighting based on secondary rainfall data in Malang Regency yielded the same results as the uniform weighting; therefore, only the uniform and inverse distance weightings were used. The generation procedure is as follows: The generation procedure is as follows:

a. Generating errors from a multivariate normal distribu-

tion with a mean vector of 0 and a variance matrix of

$$\Sigma = \begin{bmatrix} 1 & 0 & 0 \\ 0 & 1 & 0 \\ 0 & 0 & 1 \end{bmatrix}$$

b. Determining parameter values. There are 6 parameters required in the GSTAR(1, 1) model with 3 locations, namely

$$\phi_{10}^{(1)} = 0.2, \quad \phi_{10}^{(2)} = 0.25, \quad \phi_{10}^{(3)} = 0.35,$$
$$\phi_{11}^{(1)} = 0.45, \quad \phi_{11}^{(2)} = 0.33, \quad \phi_{11}^{(3)} = 0.61$$

c. Determine the value of

$$y_0 = \begin{bmatrix} 0 \\ 0 \\ 0 \end{bmatrix}$$

d. Generating y_t values based on the GSTAR(1, 1) model as in Equation (1).

$$\begin{aligned} y_{1t} &= \phi_{10}^{(1)} y_{1,t-1} + \phi_{11}^{(1)} \left(0.5 y_{2,t-1} + 0.5 y_{3,t-1}\right) + \varepsilon_{1t} \\ y_{2t} &= \phi_{10}^{(2)} y_{2,t-1} + \phi_{11}^{(2)} \left(0.5 y_{1,t-1} + 0.5 y_{3,t-1}\right) + \varepsilon_{2t} \\ y_{3t} &= \phi_{10}^{(3)} y_{3,t-1} + \phi_{11}^{(3)} \left(0.5 y_{1,t-1} + 0.5 y_{2,t-1}\right) + \varepsilon_{3t} \end{aligned} \quad (1)$$

For the simulation, the block length is based on research from (Hall et al., 1995) is $T^{1/5}$ for inference purposes and to see how the bias, confidence interval length, and variance of the parameter estimator vary with block length, block lengths of 5, 10, and 25 were also tried. The number of observations tested will be 50, 100, and 200. Meanwhile, the number of bootstrap replicates tested will be 100 and 1000.

2.2 Methods

In this study, the first step is to develop a bootstrap procedure for spatiotemporal data in the GSTAR model. The bootstrap method for spatiotemporal data was developed by adapting the bootstrap procedures for time series data, namely the Non-overlapping Block Bootstrap and the Moving Block Bootstrap. Non-overlapping Block Bootstrap for time series data can be explained as follows: Time series data can be expressed as in Equation (2).

$$\mathbf{y} = \begin{bmatrix} y_1 \\ \vdots \\ y_T \end{bmatrix} \quad (2)$$

With T being the number of periods, the matrix $\mathbf{y}$ is of size $T \times 1$. The NBB method divides the data set of size $T \times 1$ into b non-overlapping blocks $B_1, \ldots, B_b$. Each block is of size $l \times 1$ with $1 < l < T$ and $T = b\,l$. Define the non-overlapping blocks $B_1, \ldots, B_b$ of $\mathbf{y}$ as in Equation 3.

$$B_1 = \begin{bmatrix} y_1 \\ \vdots \\ y_l \end{bmatrix}, \; B_2 = \begin{bmatrix} y_{l+1} \\ \vdots \\ y_{2l} \end{bmatrix}, \; \ldots, \; B_b = \begin{bmatrix} y_{(b-1)l+1} \\ \vdots \\ y_T \end{bmatrix}. \quad (3)$$

In Moving Block Bootstrap, for a data set of size $T \times 1$, MBB divides the data set into $b = T - l + 1$ overlapping blocks of length l. The MBB block of $\mathbf{y}$ is defined as in Equation 4.

$$B_1 = \begin{bmatrix} y_1 \\ \vdots \\ y_l \end{bmatrix}, \quad B_2 = \begin{bmatrix} y_2 \\ \vdots \\ y_{l+1} \end{bmatrix}, \quad \ldots, \quad B_b = \begin{bmatrix} y_{T-l+11} \\ \vdots \\ y_T \end{bmatrix}. \quad (4)$$

After obtaining the b blocks, resampling with replacement from the blocks is performed. Combining these blocks in the order in which they were selected will produce a bootstrap sample. From the generated samples, the parameters of the time-series model (e.g., ARIMA) are estimated, and the resulting parameter estimates are stored. The bootstrap sampling and parameter estimation processes are repeated B times, producing B sets of parameter estimator and, consequently, their empirical distribution. Based on this distribution, a confidence interval for each parameter can be constructed, with the Lower Bound at the 2.5th percentile and the Upper Bound at the 97.5th percentile. This confidence interval serves as a basis for testing parameter significance. If the interval includes zero, the parameter is considered insignificant; otherwise, it is deemed significant.

Meanwhile, the GSTAR(1, 1) model with N locations can be written as in Equation 5

$$\begin{aligned} y_t &= \Phi_{10} y_{t-1} + \Phi_{11} W y_{t-1} + \varepsilon_t \\ &= \mathrm{diag}(\phi_{10}^{(1)}, \ldots, \phi_{10}^{(N)}) y_{t-1} + \mathrm{diag}(\phi_{11}^{(1)}, \ldots, \phi_{11}^{(N)}) W y_{t-1} \end{aligned} \quad (5)$$

where

$$\mathbf{y}_t = \begin{bmatrix} y_{t1} \\ \vdots \\ y_{tN} \end{bmatrix}, \qquad W = \begin{bmatrix} 0 & w_{12} & \cdots & w_{1N} \\ w_{21} & 0 & \cdots & w_{2N} \\ \vdots & \vdots & \ddots & \vdots \\ w_{N1} & w_{N2} & \cdots & 0 \end{bmatrix}$$

The parameter estimator using Ordinary Least Squares for the GSTAR(1, 1) model is given in Equation 6.

$$\boldsymbol{\beta}_i = (X_i' X_i)^{-1} X_i' \mathbf{y}_i \quad (6)$$

where

$$\boldsymbol{\beta}_i = \begin{bmatrix} \phi_{10}^{(i)} \\ \phi_{11}^{(i)} \end{bmatrix}, \qquad \mathbf{y}_i = \begin{bmatrix} y_{2i} \\ y_{3i} \\ \vdots \\ y_{Ti} \end{bmatrix},$$

$$X_i = \begin{bmatrix} y_{1i} & v_{1i} \\ y_{2i} & v_{2i} \\ \vdots & \vdots \\ y_{(T-1)i} & v_{(T-1)i} \end{bmatrix},$$

$$v_{ti} = \sum_{j=1}^{N} w_{ij} y_{tj}, \qquad i \neq j.$$

3. RESULTS AND DISCUSSION

3.1 Bootstrap Development for Spatiotemporal Data in the GSTAR Model

The bootstrap methods developed for spatiotemporal data in the GSTAR model are the Non-overlapping Block Bootstrap (NBB) and the Moving Block Bootstrap (MBB). The Moving Block Bootstrap (MBB) method is widely considered the standard in handling time series data because of its ability to preserve the dependency structure of the data, which is often broken when using traditional bootstrapping (Künsch, 1989; Lahiri, 2003). Spatiotemporal data can be expressed as in Equation (7)

$$\mathbf{Y} = \begin{bmatrix} y_1 \\ \vdots \\ y_T \end{bmatrix} = \begin{bmatrix} y_{11} & \cdots & y_{1N} \\ \vdots & \ddots & \vdots \\ y_{T1} & \cdots & y_{TN} \end{bmatrix} \tag{7}$$

With T being the number of periods and N being the number of locations, the matrix $\mathbf{Y}$ is of size $T \times N$. The NBB method divides the data set of size $T \times N$ into b non-overlapping blocks $B_1, \ldots, B_b$. Each block is of size $l \times N$ with $1 < l < T$ and $T = b \times l$. Define the non-overlapping blocks $B_1, \ldots, B_b$ of $\mathbf{Y}$ as in Equation 8.

$$B_1 = \begin{bmatrix} y_{11} & \cdots & y_{1N} \\ \vdots & \ddots & \vdots \\ y_{l1} & \cdots & y_{lN} \end{bmatrix}, \quad B_2 = \begin{bmatrix} y_{(l+1)1} & \cdots & y_{(l+1)N} \\ \vdots & \ddots & \vdots \\ y_{2l,1} & \cdots & y_{2l,N} \end{bmatrix}, \quad \ldots, \quad B_b = \begin{bmatrix} y_{((b-1)l+1),1} & \cdots & y_{((b-1)l+1),N} \\ \vdots & \ddots & \vdots \\ y_{T1} & \cdots & y_{TN} \end{bmatrix} \tag{8}$$

In Moving Block Bootstrap, for a data set of size $T \times N$, MBB divides the data set into $b = T - l + 1$ overlapping blocks of length l. The MBB blocks of $\mathbf{Y}$ are defined as in Equation 9.

$$B_1 = \begin{bmatrix} y_{11} & \cdots & y_{1N} \\ \vdots & \ddots & \vdots \\ y_{l1} & \cdots & y_{lN} \end{bmatrix}, \quad B_2 = \begin{bmatrix} y_{21} & \cdots & y_{2N} \\ \vdots & \ddots & \vdots \\ y_{(l+1)1} & \cdots & y_{(l+1)N} \end{bmatrix}, \quad \ldots, \quad B_b = \begin{bmatrix} y_{(T-l+1)1} & \cdots & y_{(T-l+1)N} \\ \vdots & \ddots & \vdots \\ y_{T1} & \cdots & y_{TN} \end{bmatrix} \tag{9}$$

After obtaining the b blocks, resampling with replacement from the blocks is performed. Combining these blocks in the order in which they were selected will produce a bootstrap sample.

From the formed sample, the parameters of the GSTAR (1,1) model are estimated, and the parameter estimates are saved. Bootstrap sample generation and parameter estimation are carried out B times, so that B sets of parameter estimates are obtained, and the distribution of the B sets of parameter estimates is obtained. From the distribution of the parameter estimator, a parameter confidence interval can be formed, namely, the Lower Bound is the 2.5th percentile, and the Upper Bound is the 97.5th percentile. This confidence interval can be used to test the significance of the parameter. If the confidence interval contains zero, the parameter is not significant; conversely, if the confidence interval does not contain zero, the parameter is significant.

Time series data have the characteristic that current values are influenced by previous values or exhibit temporal dependency; by taking data in the form of "blocks" (contiguous time sequences), this dependency relationship or pattern is preserved. Spatio-temporal data has dependencies in both the temporal and spatial dimensions. In the procedure developed in this study, one block consists of consecutive vectors $y_i, y_(i+1),\ldots$ where each vector contains all N location observations. This means that the relationship between neighbors (spatial) within a single time point is maintained because the location data is not separated during resampling.

To assess the performance of the NBB and MBB methods for spatiotemporal data in the GSTAR model, simulations are conducted, and the results are discussed in sub-chapter 3.2.

In this simulation, the GSTAR(1, 1) model with three locations and uniform weights is used. In the GSTAR(1, 1) model with 3 locations, there are 6 estimated parameters, namely $\phi_{10}^{(1)}, \phi_{10}^{(2)}, \phi_{10}^{(3)}, \phi_{11}^{(1)}, \phi_{11}^{(2)}, \phi_{11}^{(3)}$. After the simulation, the bias is presented in Table 1 to Table 6 for the NBB method and uniform spatial weight.

3.2 Simulation Results

The simulation in this study considers several things, namely, that the bootstrap method used is the Non-overlapping Block Bootstrap (NBB) and the Moving Block Bootstrap (MBB). The bootstrap replications are set to B = 100 and B = 1000. The number of observations is also taken into consideration in this simulation, with T = 50, 100, and 200 observations tried. In addition, the block length is taken into consideration, with block lengths of 5, 10, and 25 tried. In this simulation, the parameter estimator bias, confidence interval, and confidence interval width are calculated. The smaller the bias and the narrower the confidence interval, the better the bootstrap results.

Table 1 to Table 6 show that the longer the block, the smaller the bias of the parameter estimator. This applies to all parameters $\phi_{10}^{(1)}, \phi_{10}^{(2)}, \phi_{10}^{(3)}, \phi_{11}^{(1)}, \phi_{11}^{(2)}$, and $\phi_{11}^{(3)}$. Based on the number of observations (T), the more observations, the smaller the bias in the parameter estimator of $\phi_{10}^{(1)}, \phi_{10}^{(2)}, \phi_{10}^{(3)}$, but there is no pattern in the bias of the parameter estimator of $\phi_{11}^{(1)}, \phi_{11}^{(2)}$, and $\phi_{11}^{(3)}$. Based on the number of bootstrap

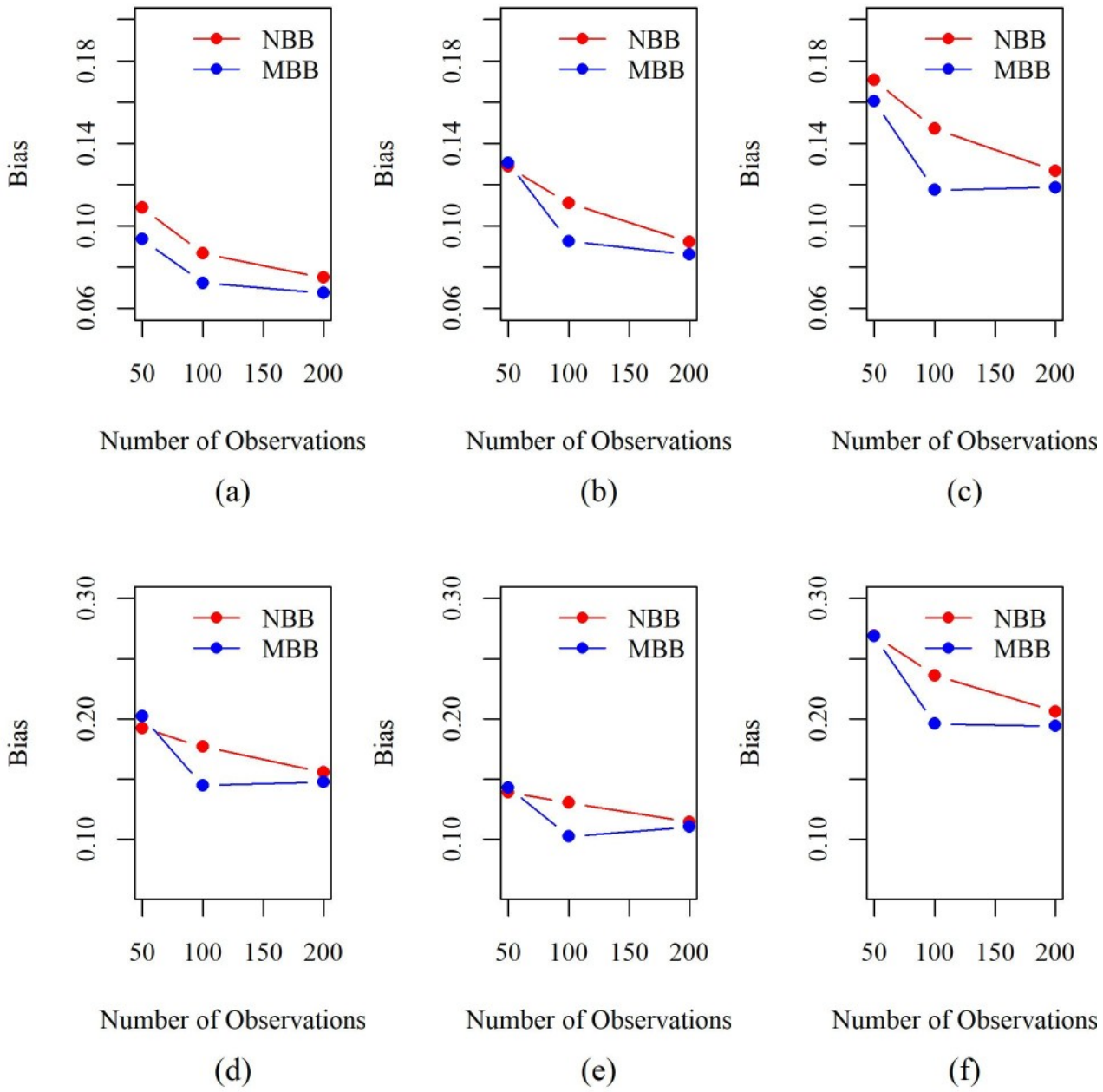

Figure 1. Plot of Bias of Parameter Estimates Using Uniform Spatial Weight: (a) $\hat{\phi}_{10}^{((1))}$, (b) $\hat{\phi}_{10}^{((2))}$, (c) $\hat{\phi}_{10}^{((3))}$, (d) $\hat{\phi}_{11}^{((1))}$, (e) $\hat{\phi}_{11}^{((2))}$, (f) $\hat{\phi}_{11}^{((3))}$

repetitions (B), the bias also does not show any pattern in the parameter estimator of $\phi_{10}^{(1)}$, $\phi_{10}^{(2)}$, $\phi_{10}^{(3)}$, $\phi_{11}^{(1)}$, $\phi_{11}^{(2)}$, and $\phi_{11}^{(3)}$.

The bias values of the parameter estimator obtained using the NBB method and inverse spatial weights are presented in Table 7 to Table 12.

The bias results for the parameter estimator of $\phi_{10}^{(1)}$, $\phi_{10}^{(2)}$, and $\phi_{10}^{(3)}$ The results presented in Tables 7-9 show that increasing the block length and the sample size (number of observations) consistently reduces bias. The use of the inverse-distance weight matrix in the GSTAR model yields a trend consistent with the findings under uniform weights.

Analysis of Tables 10-12 reveals no systematic pattern in

Table 1. Bias of the Parameter Estimator of $\phi_{10}^{(1)}$ Using the NBB Method and Uniform Spatial Weight

Block Length	B = 100			Block Length	B = 1000		
	T				T		
	50	100	200		50	100	200
$T^{1/5}$	0.1089	0.0867	0.0750	$T^{1/5}$	0.1022	0.0868	0.0750
5	0.0617	0.0546	0.0452	5	0.0593	0.0487	0.0405
10	0.0386	0.0274	0.0278	10	0.0484	0.0311	0.0249
25	0.0350	0.0236	0.0138	25	0.0286	0.0188	0.0146

Table 2. Bias of the Parameter Estimator of $\phi_{10}^{(2)}$ Using the NBB Method and Uniform Spatial Weight

Block Length	B = 100			Block Length	B = 1000		
	T				T		
	50	100	200		50	100	200
$T^{1/5}$	0.1288	0.1111	0.0922	$T^{1/5}$	0.1300	0.1070	0.0930
5	0.0800	0.0626	0.0558	5	0.0719	0.0604	0.0555
10	0.0520	0.0424	0.0297	10	0.0502	0.0343	0.0367
25	0.0405	0.0326	0.0181	25	0.0408	0.0213	0.0192

Table 3. Bias of the Parameter Estimator of $\phi_{10}^{(3)}$ Using the NBB Method and Uniform Spatial Weight

Block Length	B = 100			Block Length	B = 1000		
	T				T		
	50	100	200		50	100	200
$T^{1/5}$	0.1707	0.1472	0.1266	$T^{1/5}$	0.16607	0.1452	0.1259
5	0.0877	0.0749	0.0738	5	0.0868	0.0790	0.0742
10	0.0507	0.0472	0.0408	10	0.0517	0.0464	0.0398
25	0.0348	0.0302	0.0179	25	0.0392	0.0230	0.0221

Table 4. Bias of the Parameter Estimator of $\phi_{11}^{(1)}$ Using the NBB Method and Uniform Spatial Weight

Block Length	B=100			Block Length	B=1000		
	T				T		
	50	100	200		50	100	200
$T^{1/5}$	0.1925	0.1770	0.1557	$T^{1/5}$	0.1906	0.1755	0.1569
5	0.0869	0.0904	0.0866	5	0.0783	0.0885	0.0912
10	0.0550	0.0478	0.0440	10	0.0319	0.0450	0.0452
25	0.0152	0.0216	0.0211	25	0.0137	0.0218	0.0145

Table 5. Bias of the Parameter Estimator of $\phi_{11}^{(2)}$ Using the NBB Method and Uniform Spatial Weight

Block Length	B=100			Block Length	B=1000		
	T				T		
	50	100	200		50	100	200
$T^{1/5}$	0.1393	0.1306	0.1145	$T^{1/5}$	0.1389	0.1272	0.1106
5	0.0617	0.0639	0.0642	5	0.0654	0.0662	0.0655
10	0.0292	0.0338	0.0350	10	0.0457	0.0422	0.0336
25	0.0182	0.0120	0.0163	25	0.0295	0.0220	0.0117

Table 6. Bias of the Parameter Estimator of $\phi_{11}^{(3)}$ Using the NBB Method and Uniform Spatial Weight

Block Length	B=100			Block Length	B=1000		
	T				T		
	50	100	200		50	100	200
$T^{1/5}$	0.2694	0.2362	0.2063	$T^{1/5}$	0.2731	0.2352	0.2094
5	0.1020	0.1172	0.1192	5	0.1154	0.1168	0.1192
10	0.0673	0.0524	0.0602	10	0.0617	0.0527	0.0570
25	0.0199	0.0159	0.0258	25	0.0216	0.0234	0.0175

Table 7. Bias of the Parameter Estimator of $\phi_{10}^{(1)}$ Using the NBB Method and the Inverse Distance Spatial Weight

Block Length	B=100			Block Length	B=1000		
	T				T		
	50	100	200		50	100	200
$T^{1/5}$	0.1054	0.0841	0.0733	$T^{1/5}$	0.0997	0.0844	0.0734
5	0.0585	0.0512	0.0432	5	0.0566	0.0471	0.0380
10	0.0363	0.0289	0.0238	10	0.0341	0.0289	0.0227
25	0.0327	0.0217	0.0118	25	0.0256	0.0224	0.0113

Table 8. Bias of the Parameter Estimator of $\phi_{10}^{(2)}$ Using the NBB Method and the Inverse Distance Spatial Weight

Block Length	B=100			Block Length	B=1000		
	T				T		
	50	100	200		50	100	200
$T^{1/5}$	0.1320	0.1126	0.0932	$T^{1/5}$	0.1326	0.1086	0.0937
5	0.0833	0.0643	0.0566	5	0.0750	0.0622	0.0563
10	0.0533	0.0423	0.0353	10	0.0527	0.0361	0.0348
25	0.0425	0.0342	0.0191	25	0.0398	0.0287	0.0172

Table 9. Bias of the Parameter Estimator of $\phi_{10}^{(3)}$ Using the NBB Method and the Inverse Distance Spatial Weight

Block Length	B=100			Block Length	B=1000		
	T				T		
	50	100	200		50	100	200
$T^{1/5}$	0.1680	0.1460	0.1259	$T^{1/5}$	0.1630	0.1435	0.1254
5	0.0857	0.0742	0.0737	5	0.0849	0.0779	0.0742
10	0.0561	0.0501	0.0430	10	0.0570	0.0465	0.0398
25	0.0339	0.0303	0.0210	25	0.0428	0.0297	0.0212

the bias of the parameter estimates $\phi_{11}^{(1)}$, $\phi_{11}^{(2)}$ and $\phi_{11}^{(3)}$ under the NBB method and inverse distance spatial weighting schemes. Changes in block length, number of observations, or bootstrap replication frequency (B) do not produce a linear reduction in bias. This finding suggests that the asymptotic properties of these spatial-temporal parameter estimates may require a higher number of observations threshold or may be influenced by other data-structure factors.

The parameter estimator bias for the MBB method is presented in Table 13 to Table 18.

Table 13 to Table 15 present the bias for the parameter estimator of $\phi_{10}^{(1)}$, $\phi_{10}^{(2)}$, and $\phi_{10}^{(3)}$ using the MBB method and uniform spatial weight. These tables show that the longer the block, the smaller the bias of the parameter estimator. These tables also show that the more observations (T) there are, the smaller the estimator's bias. However, based on the bootstrap replication (B), there is no pattern of bias in the parameter estimator of $\phi_{10}^{(1)}$, $\phi_{10}^{(2)}$, and $\phi_{10}^{(3)}$.

Table 10. Bias of the Parameter Estimator of $\phi_{11}^{(1)}$ Using the NBB Method and the Inverse Distance Spatial Weight

Block Length	B=100			Block Length	B=1000		
	T				T		
	50	100	200		50	100	200
$T^{1/5}$	0.2180	0.2037	0.1842	$T^{1/5}$	0.2166	0.2027	0.1853
5	0.1262	0.1263	0.1226	5	0.1200	0.1250	0.1273
10	0.0981	0.0843	0.0866	10	0.0887	0.0867	0.0833
25	0.0623	0.0654	0.0616	25	0.0600	0.0597	0.0588

Table 11. Bias of the Parameter Estimator of $\phi_{11}^{(2)}$ Using the NBB Method and the Inverse Distance Spatial Weight

Block Length	B=100			Block Length	B=1000		
	T				T		
	50	100	200		50	100	200
$T^{1/5}$	0.0405	0.0297	0.0069	$T^{1/5}$	0.0407	0.0242	0.0011
5	0.0824	0.0747	0.0704	5	0.0733	0.0691	0.0680
10	0.1174	0.1282	0.1145	10	0.1219	0.1064	0.1127
25	0.1476	0.1510	0.1415	25	0.1300	0.1398	0.1417

Table 12. Bias of the Parameter Estimator of $\phi_{11}^{(3)}$ Using the NBB Method and the Inverse Distance Spatial Weight

Block Length	B=100			Block Length	B=1000		
	T				T		
	50	100	200		50	100	200
$T^{1/5}$	0.3152	0.2866	0.2612	$T^{1/5}$	0.3194	0.2861	0.2627
5	0.1736	0.1839	0.1855	5	0.1849	0.1844	0.1856
10	0.1207	0.1271	0.1321	10	0.1280	0.1291	0.1293
25	0.1037	0.0982	0.1023	25	0.0953	0.1048	0.1012

Table 13. Bias of the Parameter Estimator of $\phi_{10}^{(1)}$ Using the MBB Method and Uniform Spatial Weight

Block Length	B=100			Block Length	B=1000		
	T				T		
	50	100	200		50	100	200
$T^{1/5}$	0.0936	0.0724	0.0676	$T^{1/5}$	0.0936	0.0705	0.0690
5	0.0542	0.0479	0.0446	5	0.0564	0.0488	0.0419
10	0.0352	0.0323	0.0248	10	0.0366	0.0275	0.0276
25	0.0349	0.0194	0.0134	25	0.0282	0.0214	0.0129

Furthermore, the bias of the parameter estimator of $\phi_{11}^{(1)}$, $\phi_{11}^{(2)}$, and $\phi_{11}^{(3)}$ for the MBB method and uniform spatial weights are presented in Table 16, Table 17, and Table 18 respectively.

Table 16 to Table 18, which presents the bias for the parameter estimator of $\phi_{11}^{(1)}$, $\phi_{11}^{(2)}$, and $\phi_{11}^{(3)}$ using the MBB method with a uniform spatial weight, show that the longer the block, the greater the bias. This is different from the bias produced by the NBB method, where the longer the block, the smaller the bias. These tables also show no bias pattern with respect to the number of observations (T). Likewise, based on the number of bootstrap replications (B), there is no pattern for the bias of the parameter estimator of $\phi_{11}^{(1)}$, $\phi_{11}^{(2)}$, and $\phi_{11}^{(3)}$. Meanwhile, when comparing the magnitude of the bias based on the NBB and MBB methods, there is no significant difference in the bias of the parameter estimator of $\phi_{10}^{(1)}$, $\phi_{10}^{(2)}$, and $\phi_{10}^{(3)}$. However, the bias of the parameter estimator of $\phi_{11}^{(1)}$, $\phi_{11}^{(2)}$, and $\phi_{11}^{(3)}$ for

Table 14. Bias of the Parameter Estimator of $\phi_{10}^{(2)}$ Using the MBB Method and Uniform Spatial Weight

Block Length	B=100			Block Length	B=1000		
	T				T		
	50	100	200		50	100	200
$T^{1/5}$	0.1306	0.0927	0.0862	$T^{1/5}$	0.1252	0.0909	0.0862
5	0.0696	0.0568	0.0550	5	0.0688	0.0610	0.0561
10	0.0555	0.0432	0.0316	10	0.0477	0.0408	0.0321
25	0.0434	0.0341	0.0191	25	0.0404	0.0257	0.0172

Table 15. Bias of the Parameter Estimator of $\phi_{10}^{(3)}$ Using the MBB Method and Uniform Spatial Weight

Block Length	B=100			Block Length	B=1000		
	T				T		
	50	100	200		50	100	200
$T^{1/5}$	0.1605	0.1174	0.1187	$T^{1/5}$	0.1642	0.1173	0.1181
5	0.0782	0.0742	0.0753	5	0.0829	0.0801	0.0731
10	0.0708	0.0464	0.0388	10	0.0588	0.0446	0.0429
25	0.0413	0.0250	0.0219	25	0.0417	0.0330	0.0243

Table 16. Bias of the Parameter Estimator of $\phi_{11}^{(1)}$ Using the MBB Method and Uniform Spatial Weight

Block Length	B=100			Block Length	B=1000		
	T				T		
	50	100	200		50	100	200
$T^{1/5}$	0.2025	0.1448	0.1476	$T^{1/5}$	0.2034	0.1472	0.1452
5	0.2758	0.2860	0.2693	5	0.2709	0.2786	0.2724
10	0.3517	0.3562	0.3632	10	0.3442	0.3614	0.3639
25	0.4168	0.4045	0.4064	25	0.4103	0.4173	0.4089

Table 17. Bias of the Parameter Estimator of $\phi_{11}^{(2)}$ Using the MBB Method and Uniform Spatial Weight

Block Length	B=100			Block Length	B=1000		
	T				T		
	50	100	200		50	100	200
$T^{1/5}$	0.1430	0.1025	0.1105	$T^{1/5}$	0.1420	0.1070	0.1069
5	0.1965	0.1969	0.2014	5	0.1974	0.1929	0.2019
10	0.2563	0.2666	0.2618	10	0.2590	0.2544	0.2606
25	0.2777	0.2948	0.3053	25	0.3095	0.2962	0.2891

the NBB method, is smaller than the bias of the parameter estimator of $\phi_{11}^{(1)}$, $\phi_{11}^{(2)}$, and $\phi_{11}^{(3)}$ for the MBB method.

The distributions of the bias of the parameter estimator of $\phi_{10}^{(1)}$, $\phi_{10}^{(2)}$, $\phi_{10}^{(3)}$, $\phi_{11}^{(1)}$, $\phi_{11}^{(2)}$, and $\phi_{11}^{(3)}$ under the MBB procedure and inverse-distance-based spatial weighting schemes, the results are summarized in Tables 19 to 24.

Tables 13 to 15 present the bias values of the parameter estimator of $\phi_{10}^{(1)}$, $\phi_{10}^{(2)}$and $\phi_{10}^{(3)}$obtained using the Moving Block Bootstrap (MBB) method with uniform spatial weighting. These results indicate that increasing the block length and observation size (T) is positively correlated with bias reduction in the parameter estimator. In contrast, variations in the number of bootstrap replications (B) do not show a systematic pattern of influence on the bias of the parameter estimator of $\phi_{10}^{(1)}$, $\phi_{10}^{(2)}$and $\phi_{10}^{(3)}$.

As shown in Tables 22 to 24, the bias of the parameter estimator of $\phi_{11}^{(1)}$, $\phi_{11}^{(2)}$and $\phi_{11}^{(3)}$do not show any systematic trend

Table 18. Bias of the Parameter Estimator of $\phi_{11}^{(3)}$ Using the MBB Method and Uniform Spatial Weight

Block Length	B=100			Block Length	B=1000		
	T				T		
	50	100	200		50	100	200
$T^{1/5}$	0.2690	0.1960	0.1942	$T^{1/5}$	0.2747	0.1977	0.1974
5	0.3818	0.3727	0.3745	5	0.4115	0.4038	0.3760
10	0.5237	0.4932	0.4817	10	0.4958	0.5073	0.4884
25	0.5682	0.5645	0.5596	25	0.5691	0.5854	0.5695

Table 19. Bias of the Parameter Estimator of $\phi_{10}^{(1)}$ Using the MBB Method and the Inverse Distance Spatial Weight

Block Length	B=100			Block Length	B=1000		
	T				T		
	50	100	200		50	100	200
$T^{1/5}$	0.0890	0.0698	0.0651	$T^{1/5}$	0.0896	0.0673	0.0667
5	0.0363	0.0443	0.0411	5	0.0535	0.0479	0.0424
10	0.0318	0.0308	0.0207	10	0.0401	0.0213	0.0224
25	0.0258	0.0206	0.0137	25	0.0231	0.0202	0.0142

Table 20. Bias of the Parameter Estimator of $\phi_{10}^{(2)}$ Using the MBB Method and the Inverse Distance Spatial Weight

Block Length	B=100			Block Length	B=1000		
	T				T		
	50	100	200		50	100	200
$T^{1/5}$	0.1336	0.0944	0.0872	$T^{1/5}$	0.1285	0.0925	0.0870
5	0.0533	0.0612	0.0582	5	0.0752	0.0615	0.0555
10	0.0583	0.0405	0.0340	10	0.0544	0.0414	0.0325
25	0.0424	0.0282	0.0221	25	0.0495	0.0293	0.0178

Table 21. Bias of the Parameter Estimator of $\phi_{10}^{(3)}$ Using the MBB Method and the Inverse Distance Spatial Weight

Block Length	B=100			Block Length	B=1000		
	T				T		
	50	100	200		50	100	200
$T^{1/5}$	0.1569	0.1161	0.1179	$T^{1/5}$	0.1609	0.1158	0.1175
5	0.0561	0.0800	0.0742	5	0.0807	0.0707	0.0732
10	0.0593	0.0479	0.0414	10	0.0565	0.0485	0.0436
25	0.0448	0.0347	0.0207	25	0.0361	0.0217	0.0191

pattern, either in terms of block length variation or number of observations (T). A similar phenomenon is observed for the number of bootstrap replications (B), where increasing the resampling frequency does not significantly reduce bias in these parameters.

Tables 1 to 24 show the differences in dynamics between the autoregressive parameters phi sub 10 and the spatial autoregressive parameters ϕ_{11} under the NBB and MBB resampling schemes. Theoretically, the success of block bootstrapping depends heavily on satisfying the asymptotic condition that the block length should increase with the sample size (T), but at a slower rate. The simulation results in Tables 1-12 (NBB) and 13-15 (MBB) confirm this theory, where the bias decreases monotonically as block length and T increase. This is consistent with the block bootstrap principle proposed by Künsch (1989), which states that adequate block sizes can preserve the autocorrelation structure in time-series data. The irregularity of the bias pattern in ϕ_{11}, especially in Tables 22-24, under-

Table 22. Bias of the Parameter Estimator of $\phi_{11}^{(1)}$ Using the MBB Method and Inverse Distance Spatial

Block Length	B=100			Block Length	B=1000		
	T				T		
	50	100	200		50	100	200
$T^{1/5}$	0.2266	0.1756	0.1770	$T^{1/5}$	0.2277	0.1779	0.1755
5	0.0981	0.1260	0.1239	5	0.1204	0.1215	0.1257
10	0.0922	0.0852	0.0890	10	0.0835	0.0921	0.0849
25	0.0662	0.0630	0.0639	25	0.0783	0.0649	0.0642

Table 23. Bias of the Parameter Estimator of $\phi_{11}^{(2)}$ Using the MBB Method and Inverse Distance Spatial

Block Length	B=100			Block Length	B=1000		
	T				T		
	50	100	200		50	100	200
$T^{1/5}$	0.0445	0.0145	0.0006	$T^{1/5}$	0.0441	0.0071	0.0056
5	0.1174	0.0715	0.0645	5	0.0794	0.0722	0.0653
10	0.1133	0.1154	0.1215	10	0.1025	0.1113	0.1128
25	0.1428	0.1463	0.1418	25	0.1464	0.1428	0.1432

Table 24. Bias of the Parameter Estimator of $\phi_{11}^{(3)}$ Using the MBB Method and Inverse Distance Spatial

Block Length	B=100			Block Length	B=1000		
	T				T		
	50	100	200		50	100	200
$T^{1/5}$	0.3136	0.2523	0.2502	$T^{1/5}$	0.3198	0.2532	0.2527
5	0.1207	0.1811	0.1837	5	0.1696	0.1840	0.1849
10	0.1339	0.1358	0.1333	10	0.1298	0.1274	0.1302
25	0.1012	0.0984	0.1033	25	0.1031	0.1053	0.1041

scores the challenge of capturing spatial dependencies across time blocks. Theoretically, Kreiss and Lahiri (2012) explain that if the data dependency structure is more complex than the assumed block structure, then bias reduction will not occur linearly.

Simulated data show that MBB generally produces lower bias than NBB. The underlying theory is that MBB uses data more intensively with T-L+1 blocks, while NBB uses only T/L blocks. Politis (2003) stated that NBB often suffers from larger boundary effects due to discontinuities at the ends of non-overlapping blocks. This is evident in the bias values of NBB, which tend to be higher at small sample sizes than those of MBB.

This study compares uniform and inverse-distance weights to assess the sensitivity of the bootstrap method to GSTAR's spatial structure. Although the inverse distance weight matrix emphasizes heterogeneity between locations, the bias trend in the $\phi_1 0$ The parameter remains consistent with uniform weights. Based on the GSTAR theory, the consistency of the OLS estimator is maintained as long as the weight matrix is exogenous and normalized. The results of this simulation prove that the block bootstrap procedure is robust to spatial specifications as long as the temporal dependence structure within the block is maintained. Increasing the number of replications from B=100 to B=1000 had no significant impact on the bias values across the table. Theoretically, bias is the statistical expectation of the resampling distribution. According to Efron and Tibshirani (1993), increasing B will reduce the simulation variance (Monte Carlo error), but will not change the inherent bias of the resampling method towards the population parameters.

In addition to parameter estimator bias, the simulation also calculates the width of the parameter's confidence interval. The narrower the confidence interval, the better the simulation results. The width of the confidence interval for the NBB method and uniform spatial weight is presented in Table 25 to Table 30.

Table 25 to Table 30 show that by using the NBB method, the longer the block, the narrower the width of the confidence interval of the parameters of $\phi_{10}^{(1)}$, $\phi_{10}^{(2)}$, $\phi_{10}^{(3)}$, $\phi_{11}^{(1)}$, $\phi_{11}^{(2)}$, and

Table 25. Width of Confidence Interval of $\phi_{10}^{(1)}$ Using the NBB Method and Uniform Spatial Weight

Block Length	B=100			Block Length	B=1000		
	T				T		
	50	100	200		50	100	200
$T^{1/5}$	0.5161	0.3344	0.2184	$T^{1/5}$	0.5330	0.3483	0.2282
5	0.4708	0.3468	0.2510	5	0.4897	0.3609	0.2595
10	0.4185	0.3273	0.2413	10	0.4449	0.3395	0.2501
25	0.2171	0.2795	0.2243	25	0.2175	0.2920	0.2305

Table 26. Width of Confidence Interval of $\phi_{10}^{(2)}$ Using the NBB Method and Uniform Spatial Weight

Block Length	B=100			Block Length	B=1000		
	T				T		
	50	100	200		50	100	200
$T^{1/5}$	0.5122	0.3307	0.2184	$T^{1/5}$	0.5313	0.3433	0.2255
5	0.4714	0.3471	0.2499	5	0.4937	0.3638	0.2621
10	0.4344	0.3289	0.2447	10	0.4487	0.3391	0.2542
25	0.2225	0.2807	0.2276	25	0.2270	0.2925	0.2335

Table 27. Width of Confidence Interval of $\phi_{10}^{(3)}$ Using the NBB Method and Uniform Spatial Weight

Block Length	B=100			Block Length	B=1000		
	T				T		
	50	100	200		50	100	200
$T^{1/5}$	0.5094	0.3273	0.2136	$T^{1/5}$	0.5277	0.3386	0.2212
5	0.4534	0.3287	0.2385	5	0.4699	0.3449	0.2491
10	0.4020	0.3034	0.2235	10	0.4151	0.3154	0.2333
25	0.2058	0.2559	0.2048	25	0.2023	0.2668	0.2089

Table 28. Width of Confidence Interval of $\phi_{11}^{(1)}$ Using the NBB Method and Uniform Spatial Weight

Block Length	B=100			Block Length	B=1000		
	T				T		
	50	100	200		50	100	200
$T^{1/5}$	0.6748	0.4263	0.2743	$T^{1/5}$	0.7027	0.4436	0.2870
5	0.6232	0.4319	0.3094	5	0.6457	0.4555	0.3187
10	0.5634	0.4126	0.2943	10	0.6034	0.4296	0.3082
25	0.2853	0.3531	0.2702	25	0.2916	0.3635	0.2838

$\phi_{11}^{(3)}$. These tables also show that the more observations (T), the narrower the width of the confidence interval, especially at block lengths of 5 and 10, while at block length 25 at the number of observations of 50, the width of the confidence interval is narrower than when the number of observations is 100 and the width of the confidence interval at $T = 200$ is narrower than when $T = 100$. The width of the confidence intervals of the parameters of $\phi_{10}^{(1)}$, $\phi_{10}^{(2)}$, $\phi_{10}^{(3)}$, $\phi_{11}^{(1)}$, $\phi_{11}^{(2)}$, and $\phi_{11}^{(3)}$ at $B = 100$ is narrower than the width of the confidence intervals of the parameters of $\phi_{10}^{(1)}$, $\phi_{10}^{(2)}$, $\phi_{10}^{(3)}$, $\phi_{11}^{(1)}$, $\phi_{11}^{(2)}$, and $\phi_{11}^{(3)}$ at $B = 1000$.

The confidence interval width for the parameters estimated using the NBB method with inverse distance spatial weighting is presented in Table 31 to Table 36.

Referring to the data in Table 31 to Table 36 It can be seen that using the NBB method with inverse-distance spatial

Table 29. Width of Confidence Interval of $\phi_{11}^{(2)}$ Using the NBB Method and Uniform Spatial Weight

Block Length	B=100			Block Length	B=1000		
	T				T		
	50	100	200		50	100	200
$T^{1/5}$	0.6326	0.3961	0.2583	$T^{1/5}$	0.6626	0.4131	0.2675
5	0.5987	0.4130	0.2908	5	0.6287	0.4319	0.3042
10	0.5540	0.3952	0.2826	10	0.5633	0.4104	0.2954
25	0.2792	0.3358	0.2635	25	0.2836	0.3477	0.2729

Table 30. Width of Confidence Interval of $\phi_{11}^{(3)}$ Using the NBB Method and Uniform Spatial Weight

Block Length	B=100			Block Length	B=1000		
	T				T		
	50	100	200		50	100	200
$T^{1/5}$	0.8141	0.5266	0.3417	$T^{1/5}$	0.8371	0.5416	0.3525
5	0.7252	0.5199	0.3605	5	0.7439	0.5277	0.3771
10	0.6379	0.4717	0.3400	10	0.6650	0.4940	0.3524
25	0.3110	0.3796	0.3119	25	0.3215	0.4110	0.3193

Table 31. Width of Confidence Interval of $\phi_{10}^{(1)}$ Using the NBB Method and Inverse Distance Spatial Weight

Block Length	B=100			Block Length	B=1000		
	T				T		
	50	100	200		50	100	200
$T^{1/5}$	0.5168	0.3347	0.2181	$T^{1/5}$	0.5327	0.3482	0.2280
5	0.4712	0.3465	0.2515	5	0.4902	0.3617	0.2597
10	0.4155	0.3241	0.2403	10	0.4404	0.3389	0.2511
25	0.2161	0.2786	0.2241	25	0.2206	0.2895	0.2301

Table 32. Width of Confidence Interval of $\phi_{10}^{(2)}$ Using the NBB Method and Inverse Distance Spatial Weight

Block Length	B=100			Block Length	B=1000		
	T				T		
	50	100	200		50	100	200
$T^{1/5}$	0.5143	0.3323	0.2199	$T^{1/5}$	0.5338	0.3456	0.2269
5	0.4714	0.3471	0.2502	5	0.4929	0.3636	0.2623
10	0.4199	0.3290	0.2408	10	0.4516	0.3380	0.2531
25	0.2221	0.2803	0.2260	25	0.2346	0.2954	0.2347

weighting yields increasingly narrow confidence intervals. This pattern aligns with the increasing number of observations and block length. Furthermore, the estimation at $B = 100$ yields slightly narrower interval widths than $B = 1000$, although the difference is not significant.

Furthermore, the width of the confidence interval for parameters $\phi_{10}^{(1)}$, $\phi_{10}^{(2)}$, $\phi_{10}^{(3)}$, $\phi_{11}^{(1)}$, $\phi_{11}^{(2)}$, and $\phi_{11}^{(3)}$ using the MBB method and a uniform spatial weight is presented in Table 37 to Table 42.

Table 37 to Table 42, which present the confidence interval widths for $\phi_{10}^{(1)}$, $\phi_{10}^{(2)}$, $\phi_{10}^{(3)}$, $\phi_{11}^{(1)}$, $\phi_{11}^{(2)}$, and $\phi_{11}^{(3)}$ using the MBB method and a uniform spatial weight, show that the longer the block, the narrower the confidence interval. This applies to all T and all B tested. These tables also show that the confidence interval widths for the parameters $\phi_{10}^{(1)}$, $\phi_{10}^{(2)}$, $\phi_{10}^{(3)}$, $\phi_{11}^{(1)}$, $\phi_{11}^{(2)}$, and $\phi_{11}^{(3)}$ become narrower as the number of observations (T) increases. These findings are consistent with the research by

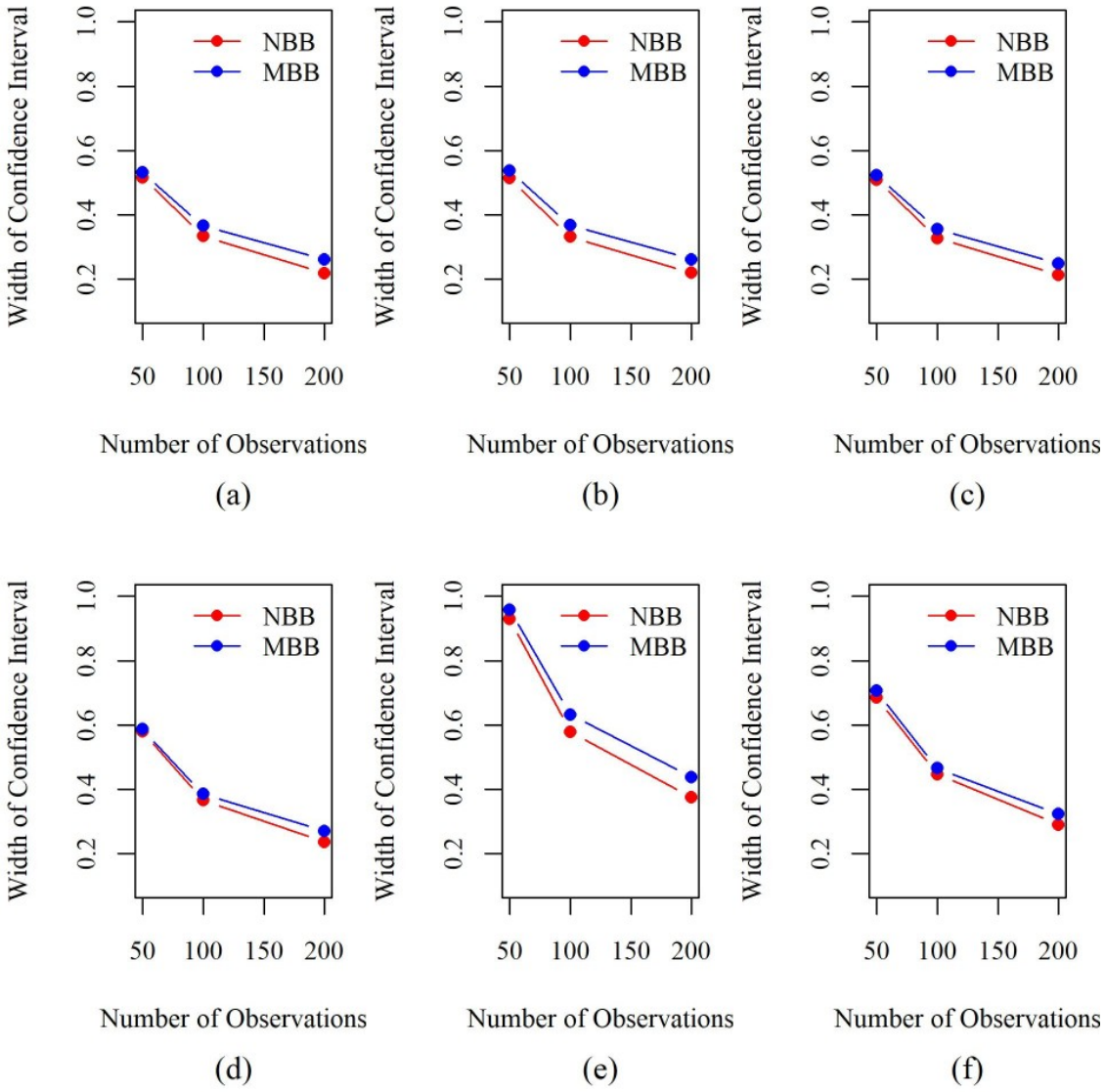

Figure 2. Plot of Bias of Parameter Estimates Using Inverse Distance Spatial Weight : (a) $\hat{\phi}_{10}^{((1))}$, (b) $\hat{\phi}_{10}^{((2))}$, (c) $\hat{\phi}_{10}^{((3))}$, (d) $\hat{\phi}_{11}^{((1))}$, (e) $\hat{\phi}_{11}^{((2))}$, (f) $\hat{\phi}_{11}^{((3))}$

Table 33. Width of Confidence Interval of $\phi_{10}^{(3)}$ Using the NBB Method and Inverse Distance Spatial Weight

Block Length	B=100			Block Length	B=1000		
	T				T		
	50	100	200		50	100	200
$T^{1/5}$	0.5092	0.3280	0.2139	$T^{1/5}$	0.5268	0.3391	0.2214
5	0.4531	0.3279	0.2377	5	0.4688	0.3447	0.2486
10	0.4011	0.3038	0.2278	10	0.4139	0.3142	0.2305
25	0.2054	0.2560	0.2048	25	0.2088	0.2691	0.2123

Table 34. Width of Confidence Interval of $\phi_{11}^{(1)}$ Using the NBB Method and Inverse Distance Spatial Weight

Block Length	B=100			Block Length	B=1000		
	T				T		
	50	100	200		50	100	200
$T^{1/5}$	0.5804	0.3660	0.2367	$T^{1/5}$	0.6012	0.3809	0.2473
5	0.5299	0.3676	0.2631	5	0.5475	0.3873	0.2712
10	0.4758	0.3489	0.2520	10	0.4922	0.3631	0.2582
25	0.2403	0.2995	0.2295	25	0.2430	0.3092	0.2402

Table 35. Width of Confidence Interval of $\phi_{11}^{(2)}$ Using the NBB Method and Inverse Distance Spatial Weight

Block Length	B=100			Block Length	B=1000		
	T				T		
	50	100	200		50	100	200
$T^{1/5}$	0.9292	0.5792	0.3757	$T^{1/5}$	0.9733	0.6016	0.3891
5	0.8851	0.6059	0.4253	5	0.9285	0.6336	0.4450
10	0.8173	0.5910	0.4188	10	0.8602	0.6021	0.4299
25	0.4136	0.4946	0.3874	25	0.4129	0.5195	0.3938

Table 36. Width of Confidence Interval of $\phi_{11}^{(3)}$ Using the NBB Method and Inverse Distance Spatial Weight

Block Length	B=100			Block Length	B=1000		
	T				T		
	50	100	200		50	100	200
$T^{1/5}$	0.6852	0.4471	0.2901	$T^{1/5}$	0.7069	0.4599	0.2998
5	0.6055	0.4345	0.3027	5	0.6216	0.4428	0.3171
10	0.5364	0.3901	0.2857	10	0.5466	0.4129	0.2972
25	0.2616	0.3178	0.2596	25	0.2733	0.3472	0.2693

Table 37. Width of Confidence Interval of $\phi_{10}^{(1)}$ Using the MBB Method and Uniform Spatial Weight

Block Length	B=100			Block Length	B=1000		
	T				T		
	50	100	200		50	100	200
$T^{1/5}$	0.5313	0.3657	0.2611	$T^{1/5}$	0.5543	0.3807	0.2707
5	0.4843	0.3503	0.2520	5	0.5032	0.3651	0.2619
10	0.4391	0.3329	0.2441	10	0.4566	0.3415	0.2501
25	0.2828	0.2875	0.2259	25	0.3006	0.2970	0.2354

Dumanjug et al. (2010), which demonstrates that an increase in the number of observations leads to a narrower confidence interval. Based on Table 37 to Table 42 It can also be seen that the interval width for bootstrap repetition $B = 100$ is narrower than that for bootstrap repetition $B = 1000$.

The confidence interval width of the parameter using the MBB method and inverse distance spatial weight is presented in Table 43 to Table 48.

Based on information from Table 43 to Table 48, a trend of narrowing confidence interval widths is observed for both the MBB and inverse-distance spatial weight methods. This occurs consistently as the number of observations and block lengths increase. The confidence interval width for B=100 appears slightly narrower than for B=1000, but the difference is not significant.

Overall, both the Non-overlapping Block Bootstrap (NBB) and Moving Block Bootstrap (MBB) methods show similar patterns in the resulting parameter confidence intervals across

Table 38. Width of Confidence Interval of $\phi_{10}^{(2)}$ Using the MBB Method and Uniform Spatial Weight

Block Length	B=100			Block Length	B=1000		
	T				T		
	50	100	200		50	100	200
$T^{1/5}$	0.5346	0.3679	0.2615	$T^{1/5}$	0.5536	0.3809	0.2708
5	0.4898	0.3541	0.2537	5	0.5091	0.3691	0.2644
10	0.4467	0.3353	0.2473	10	0.4665	0.3446	0.2546
25	0.2909	0.2941	0.2273	25	0.2940	0.2961	0.2365

Table 39. Width of Confidence Interval of $\phi_{10}^{(3)}$ Using the MBB Method and Uniform Spatial Weight

Block Length	B=100			Block Length	B=1000		
	T				T		
	50	100	200		50	100	200
$T^{1/5}$	0.5219	0.3570	0.2487	$T^{1/5}$	0.5439	0.3692	0.2604
5	0.4689	0.3379	0.2401	5	0.4856	0.3491	0.2487
10	0.4118	0.3158	0.2280	10	0.4319	0.3240	0.2358
25	0.2708	0.2594	0.2071	25	0.2786	0.2739	0.2132

Table 40. Width of Confidence Interval of $\phi_{11}^{(1)}$ Using the MBB Method and Uniform Spatial Weight

Block Length	B=100			Block Length	B=1000		
	T				T		
	50	100	200		50	100	200
$T^{1/5}$	0.6865	0.4529	0.3176	$T^{1/5}$	0.7204	0.4726	0.3298
5	1.2686	0.8793	0.6157	5	1.3144	0.9210	0.6400
10	1.1579	0.8271	0.5975	10	1.2131	0.8623	0.6251
25	0.7523	0.7253	0.5505	25	0.7704	0.7406	0.5766

Table 41. Width of Confidence Interval of $\phi_{11}^{(2)}$ Using the MBB Method and Uniform Spatial Weight

Block Length	B=100			Block Length	B=1000		
	T				T		
	50	100	200		50	100	200
$T^{1/5}$	0.6543	0.4325	0.3000	$T^{1/5}$	0.6754	0.4508	0.3106
5	1.2158	0.8412	0.5848	5	1.2507	0.8708	0.6109
10	1.1255	0.8042	0.5722	10	1.1502	0.8227	0.5985
25	0.7202	0.6930	0.5285	25	0.7532	0.7136	0.5576

various spatial weight types (uniform and inverse distance). Increasing the block length consistently narrows the width of the confidence interval. This indicates an increase in estimation precision as the data dependency structure is better captured. In the Block Bootstrap method (both NBB and MBB), the choice of block length is crucial for capturing autocorrelation or spatial/temporal dependencies. Longer blocks can capture stronger data dependencies, reducing bias in variance estimation and resulting in narrower confidence interval widths. As the number of observations increases, the width of the confidence interval narrows. This finding is in line with the Law of Large Numbers and asymptotic theory. In statistics, the standard error is inversely proportional to the square root of the number of samples. Therefore, as T increases, the variability of the estimate decreases, thereby narrowing the confidence interval. This confirms the research of Dumanjug et al. (2010), who stated that sample size is the main determinant of interval precision. Consistently across the tables, B=100 replications

Table 42. Width of Confidence Interval of $\phi_{11}^{(3)}$ Using the MBB Method and Uniform Spatial Weight

Block Length	B=100			Block Length	B=1000		
	T				T		
	50	100	200		50	100	200
$T^{1/5}$	0.8642	0.5722	0.3994	$T^{1/5}$	0.8642	0.5722	0.3994
5	1.4706	1.0248	0.7302	5	1.5446	1.0795	0.7595
10	1.3063	0.9613	0.6864	10	1.3717	0.9935	0.7066
25	0.8433	0.8076	0.6240	25	0.8791	0.8268	0.6435

Table 43. Width of Confidence Interval of $\phi_{10}^{(1)}$ Using the MBB Method and Inverse Distance Spatial Weight

Block Length	B=100			Block Length	B=1000		
	T				T		
	50	100	200		50	100	200
$T^{1/5}$	0.5313	0.3661	0.2612	$T^{1/5}$	0.5542	0.3807	0.2707
5	0.4155	0.3378	0.2441	5	0.5050	0.3664	0.2637
10	0.4239	0.3306	0.2430	10	0.4595	0.3430	0.2522
25	0.2837	0.2853	0.2244	25	0.2934	0.2947	0.2330

Table 44. Width of Confidence Interval of $\phi_{10}^{(2)}$ Using the MBB Method and Inverse Distance Spatial Weight

Block Length	B=100			Block Length	B=1000		
	T				T		
	50	100	200		50	100	200
$T^{1/5}$	0.5370	0.3691	0.2621	$T^{1/5}$	0.5561	0.3818	0.2716
5	0.4199	0.3403	0.2454	5	0.5104	0.3690	0.2666
10	0.4240	0.3335	0.2468	10	0.4567	0.3487	0.2557
25	0.2851	0.2865	0.2257	25	0.3061	0.2978	0.2368

Table 45. Width of Confidence Interval of $\phi_{10}^{(3)}$ Using the MBB Method and Inverse Distance Spatial Weight

Block Length	B=100			Block Length	B=1000		
	T				T		
	50	100	200		50	100	200
$T^{1/5}$	0.5226	0.3530	0.2487	$T^{1/5}$	0.5444	0.3687	0.2605
5	0.4011	0.3239	0.2299	5	0.4848	0.3498	0.2494
10	0.3993	0.3137	0.2251	10	0.4362	0.3236	0.2360
25	0.2683	0.2611	0.2062	25	0.2777	0.2761	0.2144

produce slightly narrower confidence intervals than B=1000, although the difference between the two is not significant. In the bootstrap literature, increasing B aims to reduce Monte Carlo error, not simply narrow the interval.

The variance of estimators $\phi_{10}^{(1)}$, $\phi_{10}^{(2)}$, $\phi_{10}^{(3)}$, $\phi_{11}^{(1)}$, $\phi_{11}^{(2)}$, and $\phi_{11}^{(3)}$ for the NBB method are presented in Table 49 to Table 54.

Table 49 to Table 54, which presents the variance of the estimators $\phi_{10}^{(1)}$, $\phi_{10}^{(2)}$, $\phi_{10}^{(3)}$, $\phi_{11}^{(1)}$, $\phi_{11}^{(2)}$, and $\phi_{11}^{(3)}$ For the NBB method, show that the longer the block, the smaller the variance. This occurs for all T and all B tested. These tables also show that the more observations (T) there are, the smaller the variance. In addition, the variances of the parameter estimates at $B = 100$ and $B = 1000$ are nearly identical.

The variance of the parameter estimates $\phi_{10}^{(1)}$, $\phi_{10}^{(2)}$, $\phi_{10}^{(3)}$, $\phi_{11}^{(1)}$, $\phi_{11}^{(2)}$ calculated using the NBB method with inverse dis-

Table 46. Width of Confidence Interval of $\phi_{11}^{(1)}$ Using the MBB Method and the Inverse Distance Spatial Weight

Block Length	B=100			Block Length	B=1000		
	T				T		
	50	100	200		50	100	200
$T^{1/5}$	0.5873	0.3854	0.2706	$T^{1/5}$	0.6161	0.4031	0.2814
5	0.4758	0.3598	0.2540	5	0.5571	0.3877	0.2739
10	0.4691	0.3521	0.2509	10	0.5083	0.3661	0.2629
25	0.3250	0.2998	0.2324	25	0.3303	0.3132	0.2435

Table 47. Width of Confidence Interval of $\phi_{11}^{(2)}$ Using the MBB Method and the Inverse Distance Spatial Weight

Block Length	B=100			Block Length	B=1000		
	T				T		
	50	100	200		50	100	200
$T^{1/5}$	0.9588	0.6325	0.4381	$T^{1/5}$	0.9908	0.6600	0.4537
5	0.8173	0.5959	0.4136	5	0.9345	0.6387	0.4502
10	0.7959	0.6009	0.4155	10	0.8592	0.6094	0.4346
25	0.5243	0.5097	0.3922	25	0.5601	0.5248	0.4152

Table 48. Width of Confidence Interval of $\phi_{11}^{(3)}$ Using the MBB Method and the Inverse Distance Spatial Weight

Block Length	B=100			Block Length	B=1000		
	T				T		
	50	100	200		50	100	200
$T^{1/5}$	0.7063	0.4654	0.3228	$T^{1/5}$	0.7316	0.4813	0.3374
5	0.5364	0.4154	0.2940	5	0.6453	0.4522	0.3166
10	0.5337	0.4300	0.2869	10	0.5742	0.4174	0.2996
25	0.3458	0.3372	0.2620	25	0.3673	0.3501	0.2714

Table 49. Variance of $\hat{\phi}_{10}^{(1)}$ Using the NBB Method and Uniform Spatial Weight

Block Length	B=100			Block Length	B=1000		
	T				T		
	50	100	200		50	100	200
$T^{1/5}$	0.0193	0.0080	0.0034	$T^{1/5}$	0.0191	0.0081	0.0034
5	0.0166	0.0088	0.0045	5	0.0167	0.0088	0.0045
10	0.0142	0.0081	0.0043	10	0.0150	0.0081	0.0042
25	0.0093	0.0066	0.0038	25	0.0097	0.0067	0.0038

tance spatial weighting is presented in Tables 55 to 60

The data in Table 55 to Table 60 reveal that the variance of the parameter estimates in the NBB method with inverse distance spatial weighting tends to decrease with increasing block length and number of observations. Furthermore, the resulting variance shows relatively stable, nearly identical values across both $B = 100$ and $B = 1000$ iterations.

Furthermore, the variance of estimators $\phi_{10}^{(1)}$, $\phi_{10}^{(2)}$, $\phi_{10}^{(3)}$, $\phi_{11}^{(1)}$, $\phi_{11}^{(2)}$, and $\phi_{11}^{(3)}$ for the MBB method and uniform spatial weights are presented in Table 61 to Table 66.

Table 61 to Table 66, which presents the variance for the estimators $\phi_{10}^{(1)}$, $\phi_{10}^{(2)}$, $\phi_{10}^{(3)}$, $\phi_{11}^{(1)}$, $\phi_{11}^{(2)}$, and $\phi_{11}^{(3)}$ For the MBB method with a uniform spatial weight, the longer the block, the smaller the variance of the estimators. These tables also show that the more observations (T) there are, the smaller the variance. This finding aligns with the results obtained from the NBB method and corroborates the research by (Duman-

Table 50. Variance of $\hat{\phi}_{10}^{(2)}$ Using the NBB Method and Uniform Spatial Weight

Block Length	B=100			Block Length	B=1000		
	T				T		
	50	100	200		50	100	200
$T^{1/5}$	0.0189	0.0079	0.0034	$T^{1/5}$	0.0189	0.0079	0.0034
5	0.0170	0.0088	0.0045	5	0.0170	0.0090	0.0046
10	0.0152	0.0081	0.0044	10	0.0152	0.0081	0.0044
25	0.0106	0.0068	0.0040	25	0.0106	0.0068	0.0039

Table 51. Variance of $\hat{\phi}_{11}^{(1)}$ Using the NBB Method and Uniform Spatial Weight

Block Length	B=100			Block Length	B=1000		
	T				T		
	50	100	200		50	100	200
$T^{1/5}$	0.0187	0.0077	0.0033	$T^{1/5}$	0.0187	0.0076	0.0032
5	0.0154	0.0079	0.0041	5	0.0154	0.0081	0.0041
10	0.0131	0.0070	0.0037	10	0.0130	0.0069	0.0037
25	0.0083	0.0056	0.0032	25	0.0084	0.0055	0.0031

Table 52. Variance of $\hat{\phi}_{11}^{(2)}$ Using the NBB Method and Uniform Spatial Weight

Block Length	B=100			Block Length	B=1000		
	T				T		
	50	100	200		50	100	200
$T^{1/5}$	0.0335	0.0131	0.0064	$T^{1/5}$	0.0334	0.0132	0.0055
5	0.0293	0.0135	0.0068	5	0.0291	0.0140	0.0068
10	0.0256	0.0128	0.0063	10	0.0276	0.0128	0.0064
25	0.0200	0.0107	0.0057	25	0.0176	0.0105	0.0057

Table 53. Variance of $\hat{\phi}_{11}^{(3)}$ Using the NBB Method and Uniform Spatial Weight

Block Length	B=100			Block Length	B=1000		
	T				T		
	50	100	200		50	100	200
$T^{1/5}$	0.0293	0.0115	0.0048	$T^{1/5}$	0.0296	0.0114	0.0048
5	0.0268	0.0124	0.0061	5	0.0274	0.0126	0.0062
10	0.0239	0.0117	0.0058	10	0.0239	0.0117	0.0059
25	0.0163	0.0097	0.0054	25	0.0166	0.0095	0.0053

jug et al., 2010) which posits that increasing the number of observations reduces the variance of parameter estimates. In addition, these tables show that the variance is almost the same across the bootstrap repetitions $B = 100$ and $B = 1000$. Based on Table 55 to Table 60, it can be seen that the variance of the estimators $\phi_{10}^{(1)}$, $\phi_{10}^{(2)}$, $\phi_{10}^{(3)}$ in the NBB method, the value is almost the same as the MBB method, while the variance of the parameter estimators $\phi_{11}^{(1)}$, $\phi_{11}^{(2)}$, and $\phi_{11}^{(3)}$ has a smaller value in the NBB method than in the MBB method.

The variance of estimators $\phi_{10}^{(1)}$, $\phi_{10}^{(2)}$, $\phi_{10}^{(3)}$, $\phi_{11}^{(1)}$, $\phi_{11}^{(2)}$, and $\phi_{11}^{(3)}$ for the MBB method and inverse distance spatial weight are presented in Table 67 to Table 72.

Based on the data in Table 67 to Table 72 It can be seen that the variance of the parameter estimates in the MBB method with inverse-distance spatial weighting tends to decrease as the block length and the number of observations increase. Furthermore, the resulting variance values are relatively stable and

Table 54. Variance of $\hat{\phi}_{10}^{(3)}$ Using the NBB Method and Uniform Spatial Weight

Block Length	B=100			Block Length	B=1000		
	T				T		
	50	100	200		50	100	200
$T^{1/5}$	0.0481	0.0200	0.0084	$T^{1/5}$	0.0474	0.0196	0.0083
5	0.0393	0.0197	0.0094	5	0.0383	0.0187	0.0095
10	0.0325	0.0165	0.0084	10	0.0332	0.0170	0.0084
25	0.0197	0.0121	0.0074	25	0.0209	0.0131	0.0072

Table 55. Variance of $\hat{\phi}_{10}^{(1)}$ Using the NBB Method and Inverse Distance Spatial Weight

Block Length	B=100			Block Length	B=1000		
	T				T		
	50	100	200		50	100	200
$T^{1/5}$	0.0193	0.0080	0.0034	$T^{1/5}$	0.0190	0.0081	0.0034
5	0.0166	0.0088	0.0045	5	0.0167	0.0089	0.0045
10	0.0140	0.0079	0.0042	10	0.0145	0.0081	0.0043
25	0.0094	0.0066	0.0038	25	0.0097	0.0066	0.0038

Table 56. Variance of $\hat{\phi}_{10}^{(2)}$ Using the NBB Method and Inverse Distance Spatial Weight

Block Length	B=100			Block Length	B=1000		
	T				T		
	50	100	200		50	100	200
$T^{1/5}$	0.0191	0.0080	0.0034	$T^{1/5}$	0.0191	0.0080	0.0034
5	0.0167	0.0088	0.0045	5	0.0169	0.0090	0.0046
10	0.0143	0.0082	0.0042	10	0.0155	0.0080	0.0044
25	0.0099	0.0068	0.0039	25	0.0108	0.0069	0.0039

Table 57. Variance of $\hat{\phi}_{10}^{(3)}$ Using the NBB Method and Inverse Distance Spatial Weight

Block Length	B=100			Block Length	B=1000		
	T				T		
	50	100	200		50	100	200
$T^{1/5}$	0.0187	0.0078	0.0033	$T^{1/5}$	0.0187	0.0077	0.0032
5	0.0154	0.0079	0.0040	5	0.0153	0.0080	0.0041
10	0.0131	0.0069	0.0038	10	0.0128	0.0069	0.0036
25	0.0083	0.0056	0.0032	25	0.0090	0.0057	0.0032

nearly identical, both at iterations B=100 and B=1000.

Based on the analysis of the data in Tables 49 and 72, a consistent pattern was found in the NBB (Non-overlapping Block Bootstrap) and MBB (Moving Block Bootstrap) methods: increasing block length reduces the variance of the parameter estimates. This applies to all scenarios of the number of observations (T) and bootstrap replications (B). The decrease in variance with increasing block length indicates that larger blocks capture spatial/temporal dependency information more effectively. This reduces the variance-estimation error that often occurs when blocks are too short (which can break the chain of correlation between data), yielding a more efficient estimator. Increasing the number of observations significantly reduces the variance. This finding is consistent across all methods and spatial weight types (uniform and inverse distance). This finding is in good agreement with the asymptotic theory and with the research of Dumanjug et al. (2010), which shows that increasing the sample size (T) reduces the standard er-

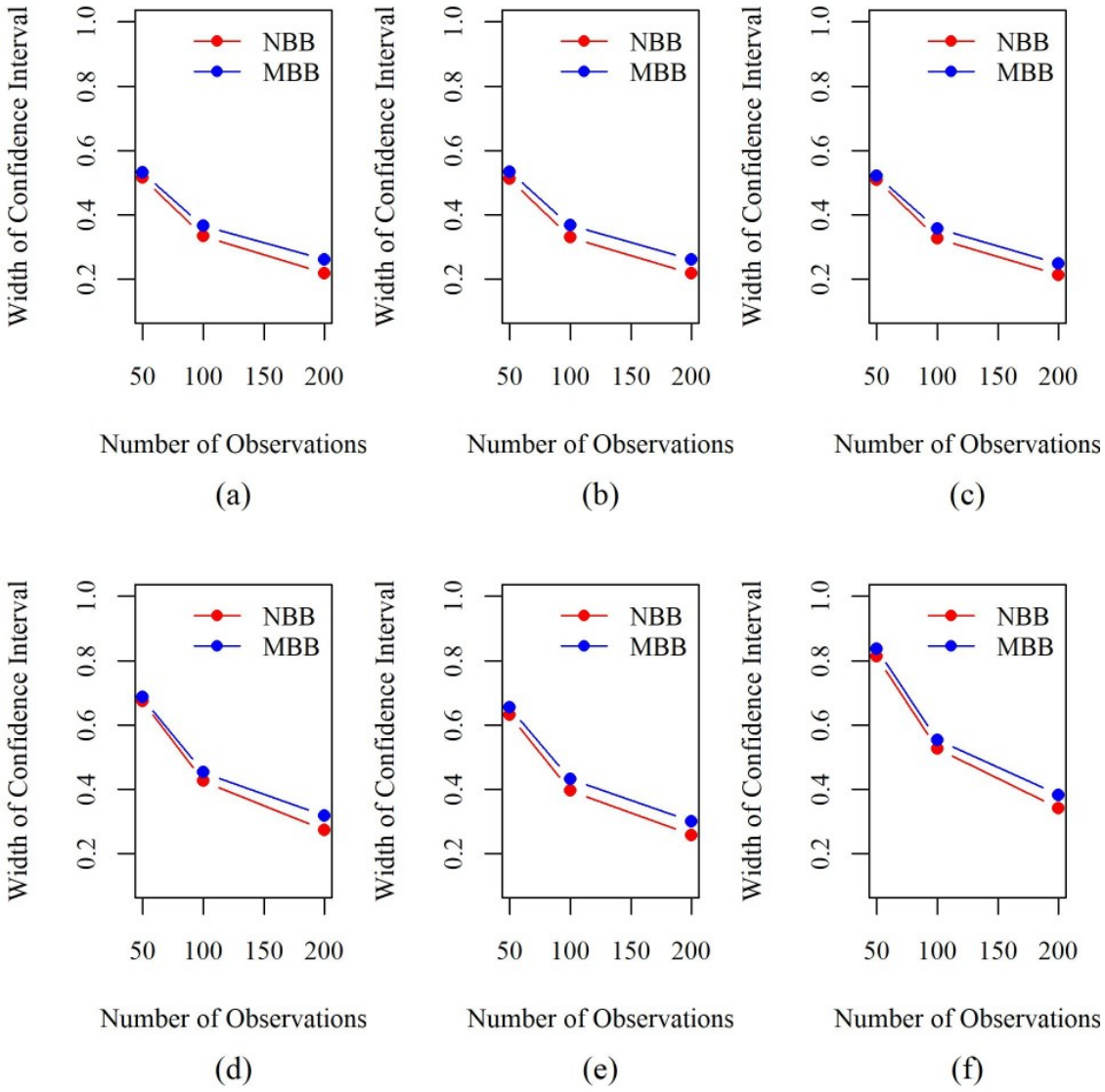

Figure 3. Plot of the Width of the Confidence Interval of the Parameter Using Uniform Spatial Weight : (a) $\phi_{10}^{((1))}$, (b) $\phi_{10}^{((2))}$, (c) $\phi_{10}^{((3))}$, (d) $\phi_{11}^{((1))}$, (e) $\phi_{11}^{((2))}$, (f) $\phi_{11}^{((3))}$

Table 58. Variance of $\hat{\phi}_{11}^{(1)}$ Using the NBB Method and Inverse Distance Spatial Weight

Block Length	B=100			Block Length	B=1000		
	T				T		
	50	100	200		50	100	200
$T^{1/5}$	0.0247	0.0097	0.0040	$T^{1/5}$	0.0244	0.0097	0.0041
5	0.0211	0.0098	0.0049	5	0.0209	0.0101	0.0049
10	0.0182	0.0091	0.0046	10	0.0182	0.0091	0.0045
25	0.0118	0.0077	0.0041	25	0.0117	0.0074	0.0041

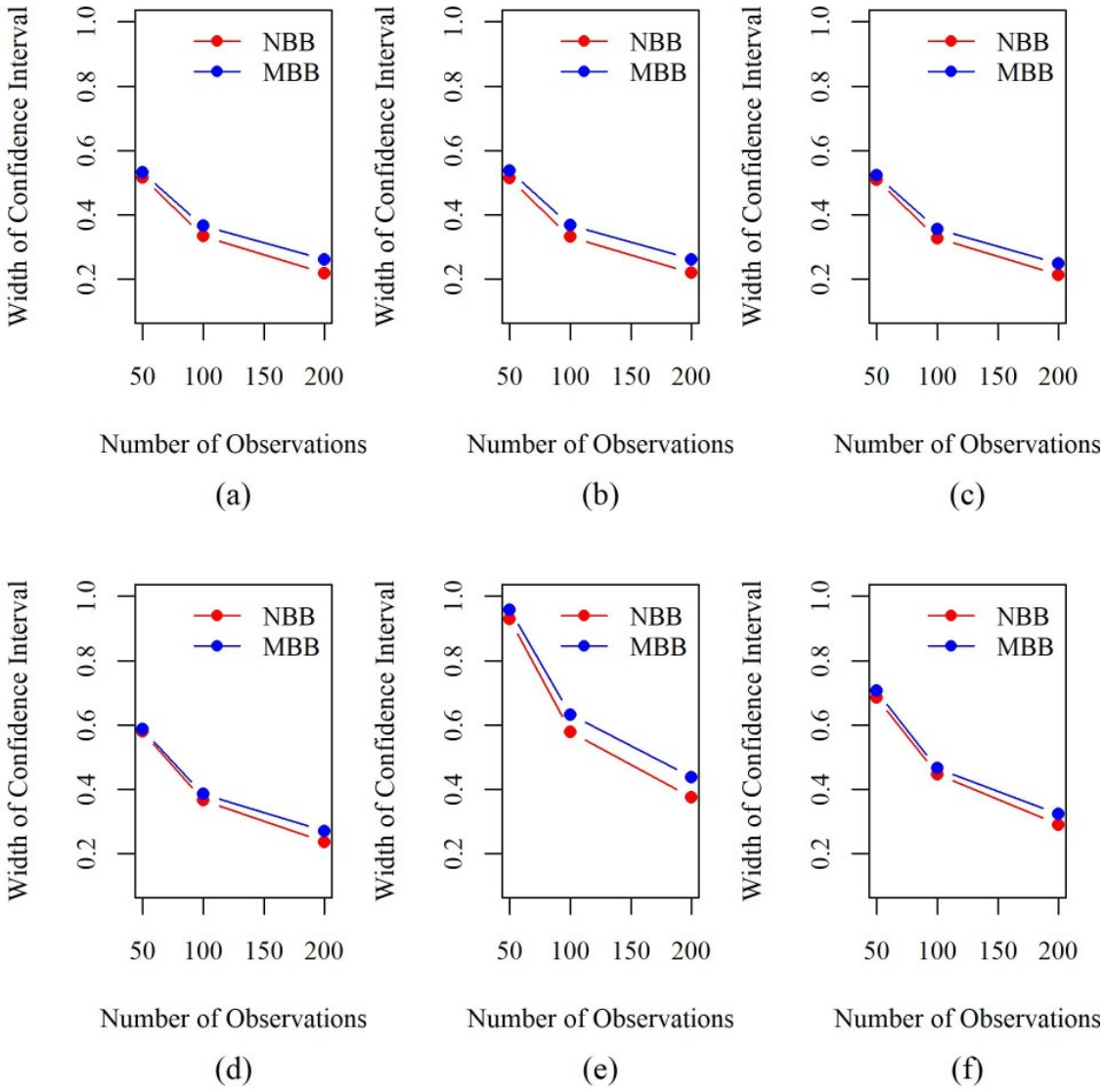

Figure 4. Plot of the Width of the Confidence Interval of the Parameter Using the Inverse Distance Spatial Weight: (a) $\phi_{10}^{((1))}$, (b) $\phi_{10}^{((2))}$, (c) $\phi_{10}^{((3))}$, (d) $\phi_{11}^{((1))}$, (e) $\phi_{11}^{((2))}$, (f) $\phi_{11}^{((3))}$

Table 59. Variance of $\hat{\phi}_{11}^{(2)}$ Using the NBB Method and Inverse Distance Spatial Weight

Block Length	B=100			Block Length	B=1000		
	T				T		
	50	100	200		50	100	200
$T^{1/5}$	0.0635	0.0245	0.0101	$T^{1/5}$	0.0642	0.0243	0.0101
5	0.0588	0.0268	0.0130	5	0.0600	0.0272	0.0132
10	0.0540	0.0264	0.0127	10	0.0558	0.0253	0.0125
25	0.0361	0.0212	0.0116	25	0.0357	0.0210	0.0110

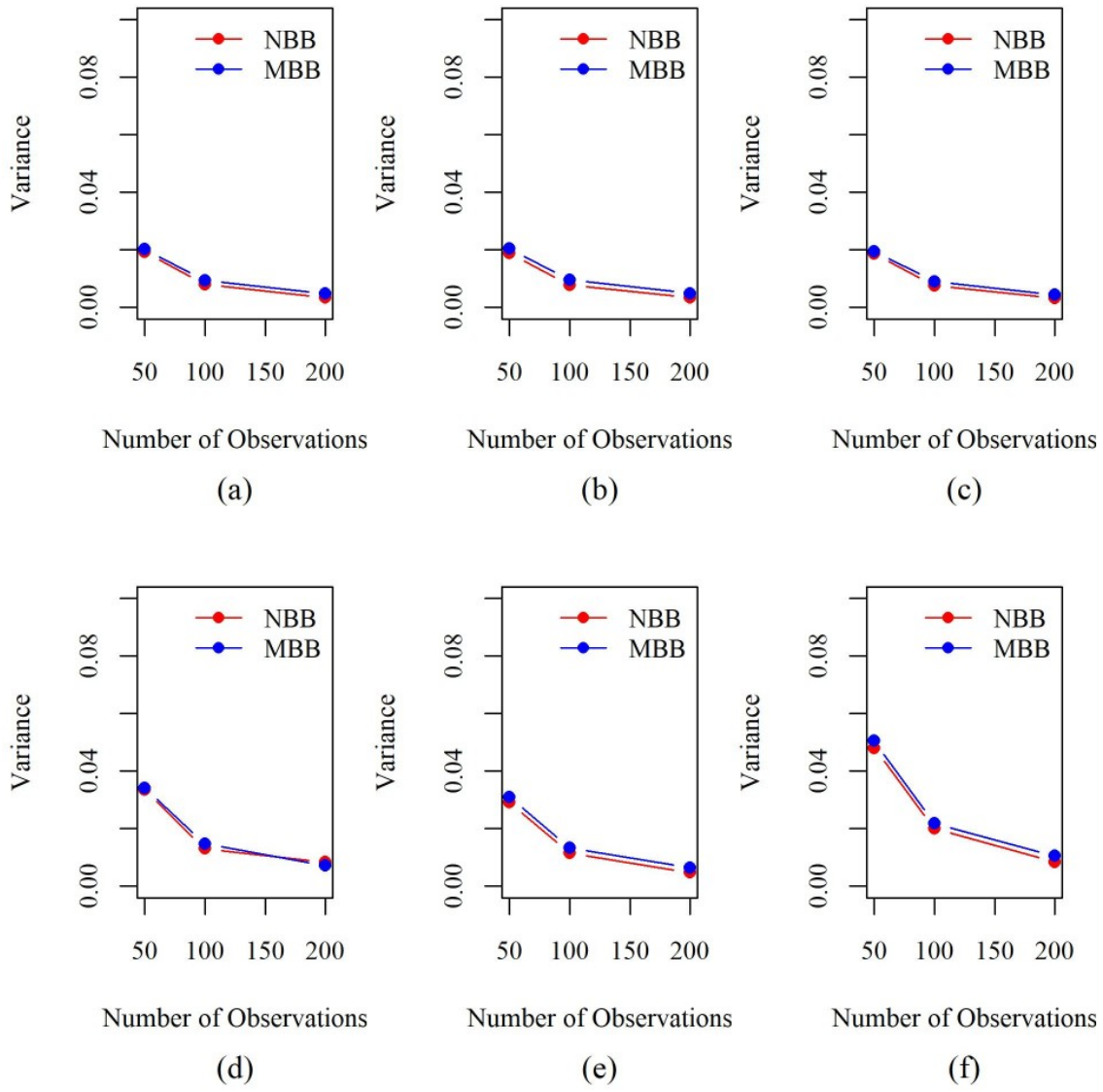

Figure 5. Plot of Variance of Parameter Estimates Using Uniform Spatial Weight: (a) $\hat{\phi}_{10}^{((1))}$, (b) $\hat{\phi}_{10}^{((2))}$, (c) $\hat{\phi}_{10}^{((3))}$, (d) $\hat{\phi}_{11}^{((1))}$, (e) $\hat{\phi}_{11}^{((2))}$, (f) $\hat{\phi}_{11}^{((3))}$

Table 60. Variance of $\hat{\phi}_{11}^{(3)}$ Using the NBB Method and Inverse Distance Spatial Weight

Block Length	B=100			Block Length	B=1000		
	T				T		
	50	100	200		50	100	200
$T^{1/5}$	0.0342	0.0144	0.0060	$T^{1/5}$	0.0337	0.0142	0.0060
5	0.0275	0.0137	0.0066	5	0.0267	0.0132	0.0067
10	0.0234	0.0114	0.0059	10	0.0225	0.0118	0.0060
25	0.0137	0.0085	0.0051	25	0.0149	0.0092	0.0052

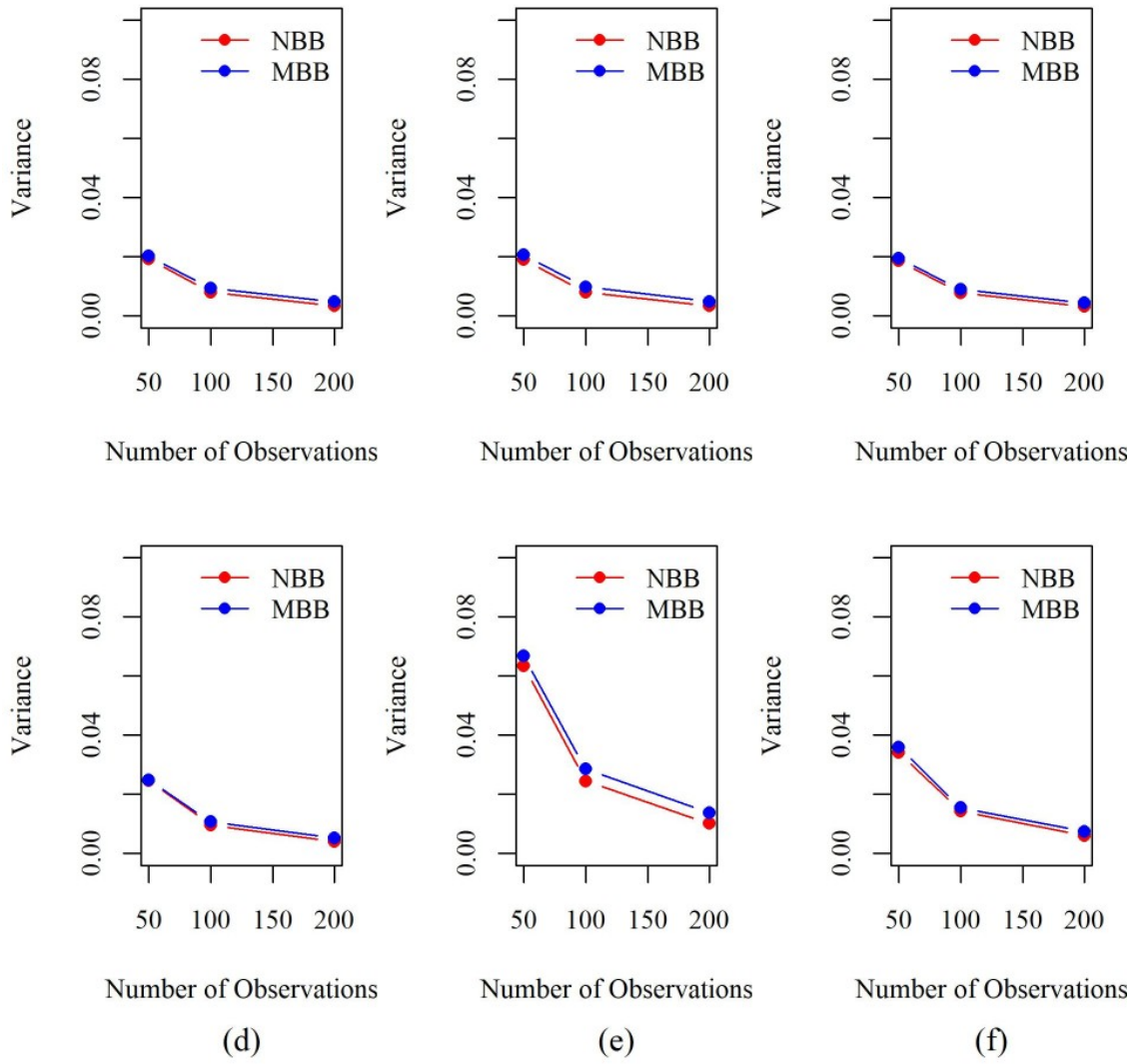

Figure 6. Plot of Variance of Parameter Estimates Using Inverse Distance Spatial Weight: (a) $\hat{\phi}_{10}^{((1))}$, (b) $\hat{\phi}_{10}^{((2))}$, (c) $\hat{\phi}_{10}^{((3))}$, (d) $\hat{\phi}_{11}^{((1))}$, (e) $\hat{\phi}_{11}^{((2))}$, (f) $\hat{\phi}_{11}^{((3))}$

Table 61. Variance of $\hat{\phi}_{10}^{(1)}$ Using the MBB Method and Uniform Spatial Weight

Block Length	B=100			Block Length	B=1000		
	T				T		
	50	100	200		50	100	200
$T^{1/5}$	0.0203	0.0095	0.0048	$T^{1/5}$	0.0204	0.0096	0.0048
5	0.0172	0.0089	0.0045	5	0.0171	0.0089	0.0045
10	0.0146	0.0081	0.0043	10	0.0146	0.0080	0.0042
25	0.0070	0.0065	0.0038	25	0.0075	0.0064	0.0038

ror. Theoretically, the variance of the estimate approaches zero as T approaches infinity. The results of this study confirm that this bootstrap model is consistent; That is, the more information (data) available, the higher the level of certainty

Table 62. Variance of $\hat{\phi}_{10}^{(2)}$ Using the MBB Method and Uniform Spatial Weight

Block Length	B=100			Block Length	B=1000		
	T				T		
	50	100	200		50	100	200
$T^{1/5}$	0.0200	0.0097	0.0049	$T^{1/5}$	0.0204	0.0096	0.0048
5	0.0175	0.0091	0.0046	5	0.0176	0.0091	0.0046
10	0.0152	0.0083	0.0044	10	0.0154	0.0081	0.0043
25	0.0074	0.0069	0.0039	25	0.0077	0.0064	0.0039

Table 63. Variance of $\hat{\phi}_{10}^{(3)}$ Using the MBB Method and Uniform Spatial Weight

Block Length	B=100			Block Length	B=1000		
	T				T		
	50	100	200		50	100	200
$T^{1/5}$	0.0196	0.0091	0.0044	$T^{1/5}$	0.0197	0.0090	0.0045
5	0.0161	0.0082	0.0041	5	0.0160	0.0081	0.0041
10	0.0130	0.0073	0.0038	10	0.0130	0.0071	0.0037
25	0.0072	0.0065	0.0036	25	0.0073	0.0062	0.0036

Table 64. Variance of $\hat{\phi}_{11}^{(1)}$ Using the MBB Method and Uniform Spatial Weight

Block Length	B=100			Block Length	B=1000		
	T				T		
	50	100	200		50	100	200
$T^{1/5}$	0.0341	0.0148	0.0072	$T^{1/5}$	0.0346	0.0148	0.0072
5	0.1180	0.0557	0.0271	5	0.1174	0.0567	0.0271
10	0.1024	0.0505	0.0258	10	0.1031	0.0506	0.0260
25	0.0504	0.0414	0.0226	25	0.0482	0.0400	0.0230

Table 65. Variance of $\hat{\phi}_{11}^{(2)}$ Using the MBB Method and Uniform Spatial Weight

Block Length	B=100			Block Length	B=1000		
	T				T		
	50	100	200		50	100	200
$T^{1/5}$	0.0310	0.0134	0.0064	$T^{1/5}$	0.0305	0.0135	0.0064
5	0.1087	0.0511	0.0245	5	0.1060	0.0506	0.0247
10	0.0966	0.0476	0.0236	10	0.0945	0.0463	0.0239
25	0.0467	0.0375	0.0208	25	0.0470	0.0362	0.0216

(lower the variability) of the parameter estimate. The variance estimates at B=100 and B=1000 are nearly identical or very stable, indicating that increasing the number of replications beyond 100 does not substantially affect the precision of the variance in this study. Although a larger B theoretically yields a smoother approximation to the distribution, the variance (as the second moment) usually converges more quickly. The results of this study indicate that 100 replications are sufficient to achieve stable variance estimates, so increasing the number to 1000 replications yields identical results but at a higher computational cost.

The comparison between the NBB and MBB methods based on the parameter estimation bias is performed through the plot visualization in Figure 1 and Figure 2. This analysis uses a block length of $T^{1/5}$ according to (Hall et al., 1995), and the number of replications B=100. The selection of B=100 is based on the finding that the bias value, confidence interval width, and variance do not differ significantly from those at

Table 66. Variance of $\hat{\phi}_{11}^{(3)}$ Using the MBB Method and Uniform Spatial Weight

Block Length	B=100			Block Length	B=1000		
	T				T		
	50	100	200		50	100	200
$T^{1/5}$	0.0506	0.0219	0.0105	$T^{1/5}$	0.0499	0.0217	0.0105
5	0.1570	0.0755	0.0380	5	0.1613	0.0777	0.0381
10	0.1284	0.0673	0.0341	10	0.1320	0.0669	0.0333
25	0.0768	0.0513	0.0284	25	0.0669	0.0333	0.0230

Table 67. Variance of $\hat{\phi}_{10}^{(1)}$ Using the MBB Method and Inverse Distance Spatial Weight

Block Length	B=100			Block Length	B=1000		
	T				T		
	50	100	200		50	100	200
$T^{1/5}$	0.0203	0.0095	0.0048	$T^{1/5}$	0.0205	0.0096	0.0048
5	0.0140	0.0089	0.0046	5	0.0173	0.0090	0.0046
10	0.0148	0.0080	0.0043	10	0.0148	0.0080	0.0043
25	0.0071	0.0064	0.0038	25	0.0069	0.0063	0.0038

Table 68. Variance of $\hat{\phi}_{10}^{(2)}$ Using the MBB Method and Inverse Distance Spatial Weight

Block Length	B=100			Block Length	B=1000		
	T				T		
	50	100	200		50	100	200
$T^{1/5}$	0.0206	0.0098	0.0049	$T^{1/5}$	0.0206	0.0097	0.0049
5	0.0143	0.0091	0.0047	5	0.0177	0.0091	0.0047
10	0.0147	0.0083	0.0044	10	0.0147	0.0083	0.0044
25	0.0072	0.0065	0.0038	25	0.0065	0.0065	0.0039

Table 69. Variance of $\hat{\phi}_{10}^{(3)}$ Using the MBB Method and Inverse Distance Spatial Weight

Block Length	B=100			Block Length	B=1000		
	T				T		
	50	100	200		50	100	200
$T^{1/5}$	0.0196	0.0090	0.0044	$T^{1/5}$	0.0197	0.0090	0.0045
5	0.0159	0.0082	0.0041	5	0.0159	0.0082	0.0041
10	0.0131	0.0072	0.0037	10	0.0134	0.0071	0.0037
25	0.0063	0.0053	0.0032	25	0.0063	0.0055	0.0032

B=1000. The bias comparison is presented in Figure 1 for uniform spatial weighting and Figure 2 for inverse distance spatial weighting, respectively.

Based on Figures 1 and 2, the MBB method tends to produce lower bias in parameter estimates than the NBB method. This pattern of MBB superiority is consistently observed, both with uniform spatial weights and with inverse-distance weights.

A comparative evaluation of the NBB and MBB methods based on the width of the parameter confidence interval is presented in Figures 3 and 4. Specifically, the comparison of the width of the confidence interval for uniform spatial weights is presented in Figure 3, while for inverse distance spatial weights is shown in Figure 4.

The visualizations in Figures 3 and 4 indicate a tendency for the NBB method to produce narrower parameter confidence intervals than the MBB method. However, the difference in confidence interval widths between the two methods does not appear to be significant.

Table 70. Variance of $\hat{\phi}_{11}^{(1)}$ Using the MBB Method and Inverse Distance Spatial Weight

Block Length	B=100			Block Length	B=1000		
	T				T		
	50	100	200		50	100	200
$T^{1/5}$	0.0249	0.0107	0.0052	$T^{1/5}$	0.0253	0.0108	0.0052
5	0.0182	0.0101	0.0050	5	0.0210	0.0100	0.0050
10	0.0180	0.0091	0.0046	10	0.0183	0.0091	0.0046
25	0.0097	0.0070	0.0040	25	0.0090	0.0072	0.0041

Table 71. Variance of $\hat{\phi}_{11}^{(2)}$ Using the MBB Method and Inverse Distance Spatial Weight

Block Length	B=100			Block Length	B=1000		
	T				T		
	50	100	200		50	100	200
$T^{1/5}$	0.0669	0.0287	0.0137	$T^{1/5}$	0.0659	0.0290	0.0136
5	0.0540	0.0279	0.0133	5	0.0594	0.0272	0.0134
10	0.0533	0.0265	0.0125	10	0.0523	0.0253	0.0126
25	0.0248	0.0208	0.0113	25	0.0260	0.0202	0.0119

Table 72. Variance of $\hat{\phi}_{11}^{(3)}$ Using the MBB Method and Inverse Distance Spatial Weight

Block Length	B=100			Block Length	B=1000		
	T				T		
	50	100	200		50	100	200
$T^{1/5}$	0.0360	0.0155	0.0075	$T^{1/5}$	0.0357	0.0154	0.0075
5	0.0234	0.0134	0.0067	5	0.0282	0.0136	0.0066
10	0.0233	0.0118	0.0059	10	0.0231	0.0118	0.0060
25	0.0103	0.0088	0.0051	25	0.0108	0.0088	0.0051

Figures 5 and 6 illustrate the comparison of parameter estimate variance between the NBB and MBB methods. A visual representation of the uniform spatial weighting scheme is shown in Figure 5, while the variance analysis for the inverse distance weighting is detailed in Figure 6.

Figures 5 and 6 indicate that the NBB method tends to produce a lower variance than MBB, although in practice the variances of the two methods are nearly identical.

To determine the statistical significance of the differences between the NBB and MBB methods, a t-test was conducted to compare bias, confidence interval width, and variance between the two methods. The detailed results of the p-value are presented in Table 73.

Based on the data in Table 73, the t-test results indicate that all p-values for the comparisons of bias, confidence interval width, and variance between the NBB and MBB methods exceed 0.05. This finding holds consistently for both uniform and inverse-distance spatial weights. Thus, there is no statistically significant difference in performance between the NBB and MBB methods.

3.3 Application on Rainfall Data

The application was conducted on rainfall data from three sub-districts in Malang Regency: Donomulyo, Bantur, and Pagak. The first step was a stationarity test using the Augmented Dickey-Fuller test. The test results are presented in Table 74.

Table 74. Shows that the p-value from the ADF test is less than 0.05 for rainfall in all three sub-districts. This indicates that rainfall in all three sub-districts is stationary.

To select the GSTAR order, three measurements are used: AIC, BIC, and HQC. The AIC, BIC, and HQC values are presented in Table 75.

Based on Table 74, The smallest BIC and HQC values are found in the GSTAR model (1.3) and the smallest AIC values are found in the GSTAR model (1.5). For simplicity, the GSTAR (1,3) model is used. Model parameter estimates are presented in Table 76, Table 77 and Table 78.

Next, the residual normality assumption was tested using the Mardia test, and the residual non-autocorrelation assumption was tested using the multivariate Portmanteau (Ljung–Box) test. The Mardia test yielded a skewness value of 9.11 (p-value

Table 73. P-Value of T-Test

Comparison	$\phi_{10}^{(1)}$	$\phi_{10}^{(2)}$	$\phi_{10}^{(3)}$	$\phi_{11}^{(1)}$	$\phi_{11}^{(2)}$	$\phi_{11}^{(3)}$
Bias (uniform)	0.3883	0.6876	0.4490	0.6644	0.5457	0.5972
Bias (Inverse Distance)	0.3383	0.7010	0.4161	0.6706	0.7386	0.5800
Width of CI (Uniform)	0.3119	0.7840	0.3367	0.3724	0.3358	0.3806
Width of CI (Inverse Distance)	0.8126	0.7869	0.8391	0.8902	0.8378	0.8881
Variance (Uniform)	0.8531	0.8175	0.8684	0.9753	0.8751	0.9034
Variance (Inverse Distance)	0.8531	0.8197	0.8760	0.9297	0.8761	0.9080

Table 74. Stationarity Test Results

Variable	p-value	Information
Rainfall in Donomulyo Sub-District	0.0100	Stationary
Rainfall in Bantur Sub-District	0.0240	Stationary
Rainfall in Pagak Sub-District	0.0100	Stationary

Table 75. AIC, BIC, and HQC Values of Several GSTAR Models

Model	AIC	BIC	HQC
GSTAR (1,1)	18.7804	18.8168	18.7938
GSTAR (1,2)	18.7172	18.7809	18.7407
GSTAR (1,3)	18.6666	18.7776	18.7202
GSTAR (1,4)	18.6848	18.8031	18.7284
GSTAR (1,5)	18.6615	18.8271	18.7352

Table 76. GSTAR(1,3) Model Parameter Estimates Equation 1

Parameter	Estimate	Standard Error	t-value	p-value
Intercept	0.0258	0.1395	0.1852	0.8540
$\phi_1^{(1)}$	0.0795	0.1489	0.5335	0.5966
$\phi_1^{(2)}$	-0.1579	0.1475	-1.0705	0.2908
$\phi_1^{(3)}$	0.2580	0.1555	1.6596	0.1048
$\phi_2^{(1)}$	0.0368	0.2365	0.1557	0.8770
$\phi_2^{(2)}$	0.0727	0.2332	0.3118	0.7568
$\phi_2^{(3)}$	0.1086	0.2442	0.4447	0.6589

= 0.52) for the asymmetry test and a kurtosis value of -1.02 (p-value = 0.31) for the peakedness test. Based on these results, the residual normality assumption is met. The results of the multivariate Portmanteau (Ljung–Box) test are presented in Table 79.

Based on Table 79, it can be seen that the p-values for all lags exceed 0.05, indicating that the non-autocorrelation assumption is met. Because the normality and non-autocorrelation assumptions are met, the GSTAR(1,3) model is suitable for rainfall forecasting in three sub-districts of Malang Regency:

Table 77. GSTAR(1,3) Model Parameter Estimates Equation 2

Parameter	Estimate	Standard Error	Nilai t	Nilai p
Intercept	0.1709	0.1589	1.0758	0.2885
$\phi_1^{(2)}$	-0.0988	0.1615	-0.6118	0.5442
$\phi_2^{(2)}$	-0.0761	0.1632	-0.4659	0.6438
$\phi_3^{(2)}$	0.0832	0.1662	0.4947	0.6236
$\phi_1^{(2)}$	-0.0544	0.2177	-0.2498	0.8041
$\phi_2^{(2)}$	-0.0839	0.2235	-0.3753	0.7094
$\phi_3^{(2)}$	0.1157	0.2272	0.5094	0.6133

Table 78. GSTAR(1,3) Model Parameter Estimates Equation 3

Parameter	Estimate	Standard Error	Nilai t	Nilai p
Intercept	-0.2288	0.1688	-1.3551	0.1830
$\phi_1^{(3)}$	-0.1174	0.1507	-0.7788	0.4407
$\phi_2^{(3)}$	-0.0417	0.1594	-0.2619	0.7948
$\phi_3^{(3)}$	-0.0151	0.1612	-0.0939	0.9256
$\phi_1^{(3)}$	0.0298	0.2341	0.1274	0.8993
$\phi_2^{(3)}$	-0.2160	0.2323	-0.9298	0.3581
$\phi_3^{(3)}$	-0.5542	0.2373	-2.3349	0.0247

Table 79. Multivariate Portmanteau Test Results

m (lag)	Q(m)	df	p-value
1	2	9	0.99
2	3.91	18	1
3	14.39	27	0.98
4	39.42	36	0.32
5	46.71	45	0.40
6	51.82	54	0.56
7	63.95	63	0.44
8	67.09	72	0.64
9	81.08	81	0.48
10	88.05	90	0.54

Donomulyo Sub-district, Pagak Sub-district, and Bantur Sub-district.

Even though the residuals are normally distributed, boot-

strapping is still carried out to assess the performance of parameter significance testing using the block bootstrap method (NBB and MBB) on the GSTAR model. The results of the bootstrap using NBB are presented in Table 80 to Table 82 and the results of the bootstrap using MBB are presented in Table 83 to Table 85.

Table 80. NBB Results Equation 1

Parameter	Estimates parameter	Standard Error	Confidence Interval
Intercept	3.6242	0.3053	3.0467 ; 4.2201*
$\phi_{10}^{(1)}$	0.0209	0.0637	-0.0999 ; 0.1549
$\phi_{20}^{(1)}$	-0.0398	0.0609	-0.1637 ; 0.0739
$\phi_{30}^{(1)}$	0.0461	0.0601	-0.0687 ; 0.1634
$\phi_{11}^{(1)}$	0.3356	0.0778	0.1677 ; 0.4835*
$\phi_{21}^{(1)}$	0.1599	0.0763	0.0179 ; 0.3183*
$\phi_{31}^{(1)}$	-0.0139	0.0686	-0.1426 ; 0.1203

Table 81. NBB Results Equation 2

Parameter	Estimates parameter	Standard Error	Confidence Interval
Intercept	3.2088	0.2683	2.7136 ; 3.7637*
$\phi_{10}^{(2)}$	0.0695	0.0587	-0.0478 ; 0.1759
$\phi_{20}^{(2)}$	0.0675	0.0568	-0.0399 ; 0.1858
$\phi_{30}^{(2)}$	0.0003	0.0479	-0.0925 ; 0.0925
$\phi_{11}^{(2)}$	0.2019	0.0528	0.1056 ; 0.3019*
$\phi_{21}^{(2)}$	0.0253	0.0512	-0.0734 ; 0.1264
$\phi_{31}^{(2)}$	0.0359	0.0429	-0.0468 ; 0.1203

Table 82. NBB Results Equation 3

Parameter	Estimates parameter	Standard Error	Confidence Interval
Intercept	3.7018	0.3047	3.1467 ; 4.2950*
$\phi_{10}^{(3)}$	0.0094	0.0752	-0.1348 ; 0.1669
$\phi_{20}^{(3)}$	-0.0629	0.0833	-0.2327 ; 0.0918
$\phi_{30}^{(3)}$	-0.0328	0.0557	-0.1355 ; 0.0727
$\phi_{11}^{(3)}$	0.2993	0.0800	0.1381 ; 0.4449*
$\phi_{21}^{(3)}$	0.1901	0.0830	0.0387 ; 0.3506*
$\phi_{31}^{(3)}$	0.0607	0.0588	-0.0507 ; 0.1740

The data presented in Table 83 to Table 85 confirm that the inference for the autoregressive parameter ϕ_{10}, ϕ_{20}, ϕ_{30} using the MBB method (the parameter is not significant because the confidence interval contains the value zero) are in line with

Table 83. MBB Result Equation 1

Parameter	Estimates parameter	Standard Error	Confidence Interval
Intercept	3.6293	0.2984	3.0798 ; 4.2342*
$\phi_{10}^{(1)}$	0.0311	0.0704	-0.1078 ; 0.1768
$\phi_{20}^{(1)}$	-0.0484	0.0615	-0.1630 ; 0.0786
$\phi_{30}^{(1)}$	0.0221	0.0655	-0.0990 ; 0.1511
$\phi_{11}^{(1)}$	0.3206	0.0820	0.1603 ; 0.4704*
$\phi_{21}^{(1)}$	0.1707	0.0773	0.0225 ; 0.3194*
$\phi_{31}^{(1)}$	0.0137	0.0746	-0.1277 ; 0.1507

Table 84. MBB Result Equation 2

Parameter	Estimates parameter	Standard Error	Confidence Interval
Intercept	3.1626	0.2558	2.6841 ; 3.6836*
$\phi_{10}^{(2)}$	0.0155	0.0567	-0.0954 ; 0.1259
$\phi_{20}^{(2)}$	0.0642	0.0513	-0.0355 ; 0.1720
$\phi_{30}^{(2)}$	-0.0046	0.0516	-0.1106 ; 0.0918
$\phi_{11}^{(2)}$	0.2596	0.0535	0.1566 ; 0.3656*
$\phi_{21}^{(2)}$	0.0369	0.0466	-0.0568 ; 0.1264
$\phi_{31}^{(2)}$	0.0283	0.0462	-0.0547 ; 0.1222

Table 85. MBB Result Equation 3

Parameter	Estimates parameter	Standard Error	Confidence Interval
Intercept	3.7332	0.2913	3.2090 ; 4.3313
$\phi_{10}^{(3)}$	0.0327	0.0723	-0.1114 ; 0.1729
$\phi_{20}^{(3)}$	-0.0478	0.0763	-0.1943 ; 0.1054
$\phi_{30}^{(3)}$	-0.0353	0.0632	-0.1573 ; 0.0833
$\phi_{11}^{(3)}$	0.2789	0.0749	0.1404 ; 0.4316*
$\phi_{21}^{(3)}$	0.1645	0.0789	0.0093 ; 0.3133*
$\phi_{31}^{(3)}$	0.0629	0.0701	-0.0743 ; 0.1960

the findings of the GSTAR analysis in Table 76 to Table 78. In contrast, the inference results for the spatial autoregressive parameters ϕ_{11}, ϕ_{21}, ϕ_{31} show differences with the GSTAR analysis, which are consistent with the results obtained from the NBB method.

In general, the findings indicate that the confidence interval inference results for the autoregressive parameters (ϕ_{10}, ϕ_{20}, ϕ_{30}) of MBB and NBB are in good agreement with the results from the GSTAR model analysis. This provides strong empirical evidence that both block bootstrap methods successfully replicate the sampling distribution of the temporal dependence of rainfall data. The use of bootstrap confidence intervals avoids

the need to assume normality of the residuals. Given that rainfall data often have skewed or non-normal distributions, the success of bootstrap CI in inferring autoregressive parameters indicates that the autoregressive parameter inference results (ϕ_{10}, ϕ_{20}, ϕ_{30}) are robust. Inferences on the spatial autoregressive parameters, based on confidence intervals in NBB and MBB that differ from the GSTAR results, indicate that the time-blocking schemes (NBB and MBB) may fail to capture spatial variability across locations.

4. CONCLUSIONS

This study concludes that the Moving Block Bootstrap (MBB) and Non-overlapping Block Bootstrap (NBB) methods satisfy the principle of asymptotic consistency, in which estimation accuracy increases with sample size and block length. Although there is no statistically significant performance difference between the two, MBB is more recommended because the overlapping block mechanism captures information more intensively and minimizes boundary effects. In its implementation, replications B=100 have reached a stable convergence point, so further increases in replication will only increase the computational burden without significant improvement in precision. This procedure is robust to various specifications of the spatial weight matrix, as long as the temporal dependence structure is maintained; however, using time-based blocks alone is found to be suboptimal for capturing complex spatial autoregressive parameters. Overall, block bootstrapping is a crucial inference tool to ensure statistical validity when the normality assumption is violated. Therefore, future research should explore the scalability of this framework on higher-order GSTAR models and develop further resampling procedures to overcome the limitations of temporal blocks in representing broader spatial dependence.

5. ACKNOWLEDGMENT

We would like to express our gratitude to the Faculty of Mathematics and Natural Sciences, Universitas Brawijaya, which has funded this research through an internal research grant (Hibah Penelitian Dana Internal) with contract number 02115.08/UN 10.F0901/B/PG/2025.

REFERENCES

Abdullah, A. S., S. Matoha, D. A. Lubis, A. N. Falah, I. G. N. M. Jaya, E. Hermawan, and B. N. Ruchjana (2018). Implementation of Generalized Space Time Autoregressive (GSTAR)-Kriging Model for Predicting Rainfall Data at Unobserved Locations in West Java. *Applied Mathematics and Information Sciences*, **12**(3); 607–615

Aprianti, A., N. Faulina, and M. Usman (2024). Generalized Space Time Autoregressive (GSTAR) Model for Air Temperature Forecasting in the South Sumatera, Riau, and Jambi Provinces. *InPrime: Indonesian Journal of Pure and Applied Mathematics*, **6**(1); 1–13

Bergström, F. (2018). *Bootstrap Methods in Time Series Analysis*. Ph.D. thesis, Stockholm University

Dumanjug, C. F., E. B. Barrios, and J. R. G. Lansangan (2010). Bootstrap Procedures in a Spatial-Temporal Model. *Journal of Statistical Computation and Simulation*, **80**(7); 809–822

Efron, B. and R. J. Tibshirani (1993). *An Introduction to the Bootstrap*. Chapman & Hall

Feng, X., W. Li, and Q. Zhu (2024). Estimation and Bootstrapping under Spatiotemporal Models with Unobserved Heterogeneity. *Journal of Econometrics*, **238**(1); 105559.

Hall, P., J. L. Horowitz, and B.-Y. Jing (1995). On Blocking Rules for the Bootstrap with Dependent Data. *Biometrika*, **82**; 561–574

Hestuningtias, F. and M. H. S. Kurniawan (2023). The Implementation of the Generalized Space-Time Autoregressive (GSTAR) Model for Inflation Prediction. *Enthusiastic International Journal of Applied Statistics and Data Science*, **3**(2); 176–188

Huda, N. M. and N. Imro'ah (2023). Determination of the Best Weight Matrix for the Generalized Space Time Autoregressive (GSTAR) Model in the COVID-19 Case on Java Island, Indonesia. *Spatial Statistics*, **54**; 100734

Härdle, W., J. Horowitz, and J.-P. Kreiss (2001). Bootstrap Methods for Time Series. Technical report

Iriany, A., Suhariningsih, B. N. Ruchjana, and Setiawan (2013). Prediction of Precipitation Data at Batu Town Using the GSTAR (1,p)-SUR Model. *Journal of Basic and Applied Scientific Research*, **3**(6); 860–865

Kreiss, J. P. and S. N. Lahiri (2012). Bootstrap Methods for Time Series. In *Handbook of Statistics*, volume 30. Elsevier, pages 3–26

Künsch, H. R. (1989). The Jackknife and the Bootstrap for General Stationary Observations. *The Annals of Statistics*, **17**(3); 1217–1241

Lahiri, S. N. (2003). *Resampling Methods for Dependent Data*. Springer Series in Statistics. Springer, New York

Landagan, O. Z. and E. B. Barrios (2007). An Estimation Procedure for a Spatial-Temporal Model. *Statistics & Probability Letters*, **77**(4); 401–406

Masteriana, D., M. I. Riani, and U. Mukhaiyar (2019). Generalized STAR (1,1) Model with Outlier: Case Study of Begal in Medan, North Sumatera. *Journal of Physics: Conference Series*, **1245**(1); 012046

Mukhaiyar, U., B. I. Bilad, and U. S. Pasaribu (2021). The Generalized STAR Modelling with Minimum Spanning Tree Approach of Weight Matrix for COVID-19 Case in Java Island. *Journal of Physics: Conference Series*, **2084**(1); 012003

Mukhaiyar, U., N. M. Huda, R. R. K. Novita Sari, and U. S. Pasaribu (2019). Modeling Dengue Fever Cases by Using GSTAR(1;1) Model with Outlier Factor. *Journal of Physics: Conference Series*, **1366**(1); 012122

Mukhaiyar, U., N. M. Huda, K. N. Sari, and U. S. Pasaribu (2020). Analysis of Generalized Space Time Autoregressive with Exogenous Variable (GSTARX) Model with Outlier Factor. *Journal of Physics: Conference Series*, **1496**(1); 012004

Mukhaiyar, U., A. W. Mahdiyasa, K. N. Sari, and N. T. Noviana (2024). The Generalized STAR Modeling with Minimum Spanning Tree Approach of Spatial Weight Matrix. *Frontiers in Applied Mathematics and Statistics*, **10**; 1417037

Mukhaiyar, U. and S. Ramadhani (2022). The Generalized STAR Modeling with Heteroscedastic Effects. *CAUCHY: Journal of Pure and Applied Mathematics*, **7**(2); 158–172

Nainggolan, N. and J. Titaley (2017). Development of Generalized Space Time Autoregressive (GSTAR) Model. In *AIP Conference Proceedings*, volume 1827. page 020034

Nurhayati, N., U. S. Pasaribu, and O. Neswan (2012). Application of Generalized Space-Time Autoregressive Model on GDP Data in West European Countries. *Journal of Probability and Statistics*

Politis, D. N. (2003). The Impact of Bootstrap Methods on Time Series Analysis. *Statistical Science*, **18**(2); 219–230

Prillantika, J. R., E. Apriliani, and N. Wahyuningsih (2018). Comparison between GSTAR and GSTAR-Kalman Filter Models on Inflation Rate Forecasting in East Java. *Journal of Physics: Conference Series*, **974**; 012039

Ruchjana, B. N. (2002). *A Generalized Space-Time Autoregressive Model and Its Application to Oil Production*. Ph.D. thesis, Institut Teknologi Bandung

Ruchjana, B. N., S. A. Borovkova, and H. P. Lopuhaa (2012). Least Squares Estimation of Generalized Space Time AutoRegressive (GSTAR) Model and Its Properties. In *AIP Conference Proceedings*, volume 1450. pages 61–64

Setiawan, Suhartono, and M. Prastuti (2016). S-GSTAR-SUR Model for Seasonal Spatio Temporal Data Forecasting. *Malaysian Journal of Mathematical Sciences*, **10**(S); 53–65

Suhartono, S. R. Wahyuningrum, Setiawan, and M. S. Akbar (2016). GSTARX-GLS Model for Spatio-Temporal Data Forecasting. *Malaysian Journal of Mathematical Sciences*, **10**(S); 91–103

Yundari, U. S. Pasaribu, U. Mukhaiyar, and M. N. Heriawan (2018). Spatial Weight Determination of GSTAR(1;1) Model by Using Kernel Function. *Journal of Physics: Conference Series*, **1028**(1); 012223

Zewdie, M. A., G. G. Wubit, and A. W. Ayele (2018). G-STAR Model for Forecasting Space-Time Variation of Temperature in Northern Ethiopia. *Turkish Journal of Forecasting*, **2**(1); 9–19

